IZMIR KATIP CELEBI UNIVERSITY

GRADUATE SCHOOL OF NATURAL AND APPLIED SCIENCES

ESTIMATION OF ANNUAL ENERGY PRODUCTION OF COUPLED VERTICAL-AXIS WIND TURBINES IN A SEMI-COMPLEX TERRAIN

M.Sc. THESIS

Ferhat Cem BAŞER

Department of Mechanical Engineering

JUNE 2019

IZMIR KATIP CELEBI UNIVERSITY

GRADUATE SCHOOL OF NATURAL AND APPLIED SCIENCES

ESTIMATION OF ANNUAL ENERGY PRODUCTION OF COUPLED VERTICAL-AXIS WIND TURBINES IN A SEMI-COMPLEX TERRAIN

M.Sc. THESIS

Ferhat Cem BAŞER
Y170217001

Department of Mechanical Engineering

Thesis Advisor: Asst. Prof. Dr. Ziya Haktan Karadeniz

JUNE 2019

İZMİR KATİP ÇELEBİ ÜNİVERSİTESİ

FEN BİLİMLERİ ENSTİTÜSÜ

EŞLİ ÇALIŞAN DÜŞEY EKSENLİ RÜZGAR TÜRBİNLERİNİN YARI KARMAŞIK BİR SAHADAKİ YILLIK ENERJİ ÜRETİMİNİN DEĞERLENDİRİLMESİ

YÜKSEK LİSANS TEZİ

Ferhat Cem BAŞER
Y170217001

Makina Mühendisliği Ana Bilim Dalı

Tez Danışmanı: Dr. Öğr. Üyesi Ziya Haktan Karadeniz

HAZİRAN 2019

Ferhat Cem BAŞER, a **M.Sc.** student of **IKCU Graduate School Of Natural And Applied Sciences**, successfully defended the thesis entitled "**ESTIMATION OF ANNUAL ENERGY PRODUCTION OF COUPLED VERTICAL-AXIS WIND TURBINES IN A SEMI-COMPLEX TERRAIN**", which he prepared after fulfilling the requirements specified in the associated legislations, before the jury whose signatures are below.

Thesis Advisor :

        Asst. Prof. Dr. Ziya Haktan Karadeniz
        İzmir Kâtip Çelebi University

Jury Members :

        Asst. Prof. Dr. Sercan Acarer
        İzmir Kâtip Çelebi University

        Asst. Prof. Dr. Ferhat Bingöl
        Izmir Institute of Technology

Date of Submission : 11.06.2019
Date of Defense   : 20.06.2019

To my family and my beloved,

FOREWORD

First and foremost, I would like to thank my advisor, Asst. Prof. Dr. Ziya Haktan Karadeniz, Assoc. Prof. Dr. Alpaslan Turgut and İskender Kökey. I am greatful to my family and my friends for their support during the making of this thesis.

June 2019

Ferhat Cem BAŞER

TABLE OF CONTENTS

x

ABBREVIATIONS

WRA	**:** Wind Resource Assessment
HAWT	**:** Horizontal Axis Wind Turbine
VAWT	**:** Vertical Axis Wind Turbine
PWD	**:** Prevailing wind direction
WAsP	**:** Wind Atlas Analysis and Application Program
TI	**:** Turbulence intensity

LIST OF TABLES

ESTIMATION OF ANNUAL ENERGY PRODUCTION OF COUPLED VERTICAL-AXIS WIND TURBINES IN A SEMI-COMPLEX TERRAIN

ABSTRACT

Recent research shows that the vertical-axis wind turbines (VAWTs) can provide up to 6 - 9 times more power generation in the same footprint area when they are sited in proper configurations in contrast to horizontal-axis wind turbines (HAWT). In order to site wind turbines in a field, it is necessary to do a wind resource assessment (WRA). This assessment provide important inputs for the placement, sizing and design detailing of the wind farm. In addition to the correct determination of the site, it is also critical to place the wind turbines in the most efficient way. When the necessary data are provided to a software developed for this subject, the annual energy production (AEP) calculations can be made realistically. However, these programs are designed for HAWTs. Although there is no study conducted on VAWTs using these software packages, it is possible to calculate the AEP by simply defining a turbine power curve. In the case of coupled turbines, wake effect created by the turbines affect the performance of the wind turbines, thus the total annual energy production of the turbines is a function of the wind direction. For this reason, annual energy production of the turbines should be calculated by taking into consideration the change of wind direction during the year. In this study, firstly, the field performance of two VAWTs, which are separated, were investigated. In addition, a method has been proposed in order to place the coupled VAWTs in a wind farm and calculate their AEP. It was found that the turbines operating in this method could show performance increase from 2% to 10% compared to seperated ones.

EŞLİ ÇALIŞAN DÜŞEY EKSENLİ RÜZGAR TÜRBİNLERİNİN YARI KARMAŞIK BİR SAHADAKİ YILLIK ENERJİ ÜRETİMİNİN DEĞERLENDİRİLMESİ

ÖZET

Son araştırmalar, düşey eksenli rüzgar türbinlerinin (DERT), yatay eksenli rüzgar türbinlerine (YERT) göre, uygun dizilimlerle sahaya yerleştirildiklerinde, aynı birim alanda 6 - 9 kat daha fazla güç üretimi sağlayabileceğini göstermektedir. Bir alana rüzgar türbinleri yerleştirmek için bir rüzgar kaynağı değerlendirmesi (RKD) yapılması gerekmektedir. Bu değerlendirme, rüzgar tarlasının yerleştirilmesi, boyutlandırılması ve tasarım detaylandırması için önemli girdiler sağlar. Sahanın doğru tespitine ek olarak, rüzgar türbinlerini en verimli şekilde yerleştirmek de önemlidir. Bu konuda geliştirilen bir yazılıma gerekli veriler sağlandığında, yıllık enerji üretimi (YEÜ) hesaplamaları gerçekçi bir şekilde yapılabilmektedir. Fakat bu programlar YERT'ler için tasarlanmıştır. Bu yazılım paketlerini kullanarak DERT'ler üzerinde yapılmış bir çalışma bulunmamasına rağmen, sadece türbin güç eğrisi tanımlanarak YEÜ hesaplanması mümkündür. Eşli çalışan türbinlerde ise türbinlerin arkalarında bıraktıkları rüzgar gölgeleri performansı etkilediğinden, türbinlerin toplam yıllık enerji üretimi rüzgar geliş yönünün bir fonksiyonudur. Bu nedenle türbinlerin yıllık enerji üretimi yıl boyunca rüzgar geliş yönünün değişimi göz önünde bulundurularak hesaplanmalıdır. Bu çalışmada, öncelikle ayrık çalışan iki DERT'in saha performansı incelenmiştir. Ayrıca etkileşim halinde eşli çalışan DERT'lerin bir rüzgar tarlasına yerleştirilmesi ve YEÜ hesaplanabilmesi için bir yöntem önerilmiştir. Bu yöntem kullanılarak yapılan analizlerde eşli çalışan türbinlerin, ayrık çalışanlara göre YEÜ bakımından %2'den %10'a kadar performans artışı gösterebileceği bulunmuştur.

1. INTRODUCTION

The limited fossil energy resources and the increase of carbon emission in the atmosphere and oceans are becoming a threat to the world as the global energy demand and the global fossil fuel consumption increase. This issue leads the world to find alternative energy resources. Thus, renewable energy resources is becoming more and more promising and reliable with the technological progress in this industry. One of the latest statistical reports tells that [1], renewable power grew by 17%, higher than the 10-year average and the largest increment on record (69 mtoe) in 2017 and among these, wind provided more than half of renewables growth, while solar contributed more than a third despite accounting for just 21% of the total. According to the statistics published by World Wind Energy Association, the overall capacity of all wind turbines installed worldwide by the end of 2018 has reached 600 GW [2]. Therefore, the wind energy market holds a promising position.

The energy available in the wind is proportional to the cube of wind speed. For this reason, even the slightest alterations of the wind speed can change the energy output greatly. Because of this physical law, wind energy resource developers look for high wind resource sites and place the turbines where they can harvest the maximum amount of the available energy in the wind.

As the wind speed increases, the amount of area required per unit energy production increases. The studies on the Darrieus type wind turbines that work as coupled and placed in groups show that this value can be reduced to 2 - 4 times, and the power density per floor area can be increased up to 20 W/m^2 for wind speed of 10 m/s (Figure 1.1) [3;4].
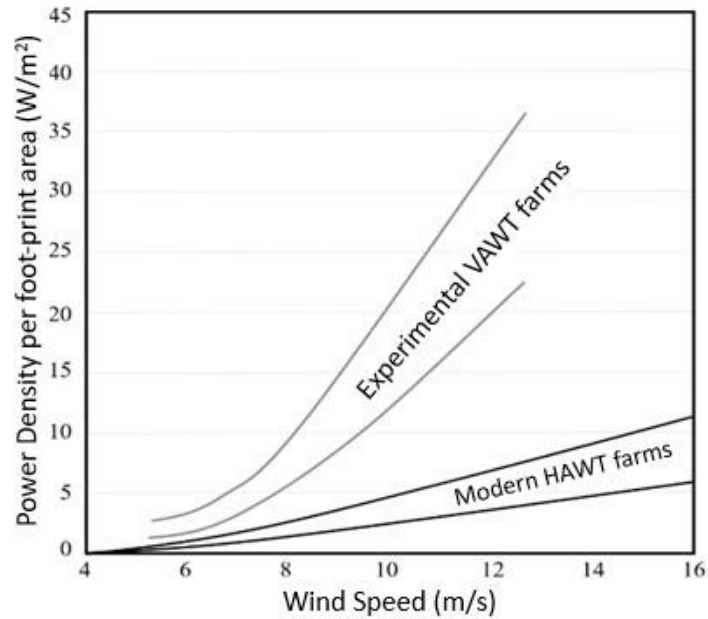
Figure 1.1 : Change of power density (W/m^2) per foot-print area versus the mean wind speed (m/s) [3].

This study proposes a method for determining the annual energy production of a pair of coupled VAWTs in a software suitable for HAWTs. The proposed method has not been previously tried in the literature and it is foreseen that the study result will lead to the dissemination of the analysis of paired VAWTs.

1.1 Vertical Axis Wind Turbines

Most wind turbine plants consist of huge horizontal axis wind turbines (HAWTs). This is because they have high mechanical power output. However, when HAWTs are placed close to each other, the wake they create behind has a negative effect on each other's power coefficients. Therefore, they need to be placed far apart from each other and are fundamentally limited by the availability of land. In addition, since the near-ground wind is turbulent HAWTs are installed high above the ground, making them harder to reach for repairs and maintenance.

Unlike HAWTs, vertical axis wind turbines (VAWTs) are capable of catching the wind from all directions; hence do not need yaw mechanisms. They have low sound emissions [5] and better performance in skewed flow [6]. Since their generators close to the ground, it is easy to access for repairs and maintenance.

1.1.1 Paired VAWTs

The power factor of a stand-alone VAWT is much lower than that of HAWT and is more expensive than HAWT with similar rated power. Considering the high-energy needs of today's world, the large number of electricity generation with high efficiency is a priority, so the number of studies on the VAWTs is very low compared to the number of studies related to HAWTs. In the latest research [4;7;8;16], there has been a change in the electricity generation approaches from wind energy when the phenomena of increasing the VAWT efficiency associated with the concept of energy density per floor area and the paired (coupled) VAWT arrays are combined. In a pioneering study [4] on the increase in power density of wind farms with paired VAWT arrays, it was experimentally demonstrated under real wind conditions that these turbine arrays perform 6 - 9 times better than today's HAWT sites. The power plant area can be used more efficiently because one turbine can catch the energy that cannot be caught by the other turbine when they are placed close to each other in a specific array [16].

In Dabiri's study [4], two counter rotating VAWTs, separated by 1.65 turbine diameter, were examined. Clockwise-rotating turbine was rotated around the azimuth of counter-clockwise-rotating turbine and measured at multiple locations in order to ascertain the relation of turbine performance with the effect of the direction of the wind. A normalized power coefficient was defined to evaluate the performance of each configuration. The results showed that the performance of the turbines slightly improved compared to isolated ones. Also, the outcome of this experiment appeared to be similar to the previously made simplified numerical models [16].

1.2 Wind Resource Assessment

In order to site wind turbine fields and even a single wind turbine, it is necessary to know the characteristics of the land, wind direction and speed. In order to answer the questions of "how much energy?" or "how much capacity?", wind resource assessment (WRA) is of great importance. Wind resource assessment is the process of calculating the wind resource or wind power potential on one or more areas. This evaluation can be done with various computer software. These assessments provide important inputs for the placement, sizing and design detailing of the wind farm. In addition to the correct determination of the site, it is also critical to place the wind turbines in the most

efficient way. Thus, it can be determined how much of the potential in the field can be converted into electrical energy with the turbines used. When the necessary data is provided to the software developed for this subject, the calculations can be made with moderate accuracy. However, with only a large proportion of these software packages designed for HAWTs (e.g. WAsP, WindPRO and WindSim), it is only partially possible to work on VAWTs.

1.2.1 Phases of WRA

As above-mentioned WRA is the process of calculating the wind power potential of a field and it can be divided into three main parts;

a) Initial site selection

b) Site wind resource evaluation

c) Micrositing

Selection of the site mostly depends on the local conditions; topography, obstacles around the site that can block the wind flow and roughness of the ground. On-shore wind turbine fields mostly sited in open and flat terrains in order to get the most energy from the wind flow. It is also important to have the wind turbine plant in a site that has high wind resource.

Evaluation of the wind resource is highly effective on the estimation of AEP of a plant. Measurement of the wind data must be done as described in IEC-61400-12-1. The measurement equipment must be arranged appropriately. One of the most important factor is that the anemometer and the wind vane must be positioned closest to the hub-height of turbine to be used. Other equipments like thermometers and pressure sensors should be positioned where they cannot hinder the anemometer and the wind vane.

Another thing that has to be taken into consideration is micrositing. Having the turbines sited in the most efficient way dramatically increases the power output. For example, the conventional HAWTs must be positioned far apart from each other in order to avoid the aerodynamic interactions between their wakes. Whereas, in the light of the recent research [4;7;8;16] VAWTs perform better when they are positioned very close to each other in a specific order.

4

1.2.2 WAsP software

WAsP (Wind Atlas Analysis and Application Program) is a broadly used software for estimating the wind energy resources [9]. It is based on the wind atlas method as described in [10]. The wind atlas method uses statistical methods to eliminate the effects of obstacles, roughness lengths of the area and the topography to convert the Weibull probability distribution of the wind data into simplified wind statistics. WAsP then applies these wind statistics to the prediction area assuming that the measurements are taken place within the same climate region. Hereby, the effects of roughness lengths, obstacles and topography are implemented to the generalized wind statistics. Lastly, Weibull probability distribution of the area is calculated [11]. Although the program is based on atmospheric conditions which are predominantly neutrally stable, empirical corrections for mildly non-neutral conditions may also be applied through manipulation of the WAsP parameters [9].

In this study, WAsP 10 is used for analyses. WAsP 10 has a couple of built-in tools to create related files in order to make calculations. Some of are:

    a) WAsP Climate Analyst (Figure 1.2)

    b) Turbine Editor Tool (Figure 1.3)

    c) Map Editor (Figure 1.4)

WAsP needs 3 main inputs to do analyses. A vector map of the area which contains roughness lengths of the site, obstacles around the turbine field and the topographic data, an observed mean climate analysis of the prediction site and a turbine power curve for a specific air density. Maps, observed wind climates and wind turbine generators cannot be created or edited from within the WAsP application so their corresponding files must be established beforehand using the Map Editor, the Climate Analyst and the Turbine Editor, respectively. Vector maps can be obtained digitally from platforms such as www.earthexplorer.usgs.gov and can be modified using softwares such as Global Mapper. After that, roughness lengths can be added using Map Editor tool. Lastly, met. mast, turbine and obstacle locations can be arranged in WAsP application.

In this study, WAsP 10 and Global Mapper 18 is used along with WAsP Climate Analyst 3, Map Editor 12 and Turbine Editor 10.
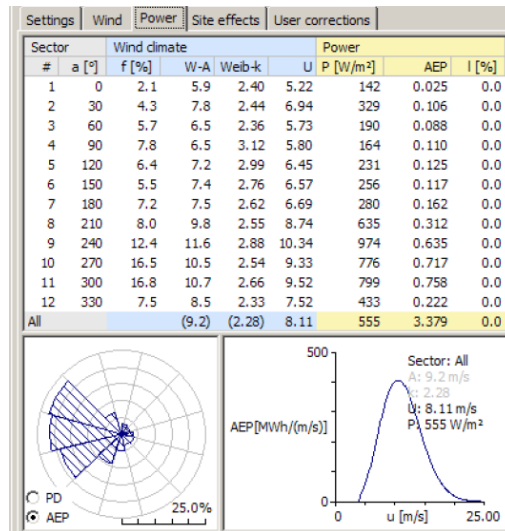
Figure 1.2 : A view from Climate Analyst.
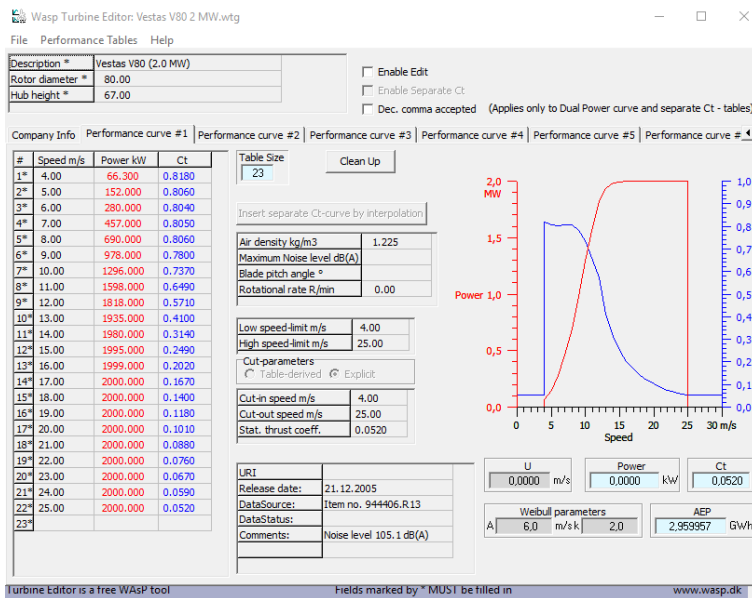
Figure 1.3 : A view from Turbine Editor.
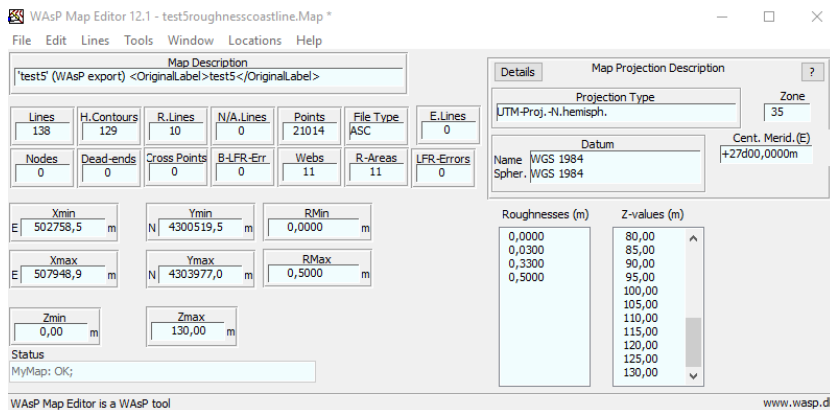
Figure 1.4 : A view from Map Editor.

2. MATERIALS AND METHODS

2.1 Turbine Specifications

The turbine used in this study is currently commercially available and it is named Mariah Windspire 1.2 kW. The turbine has a rotor diameter of 1.2 m and a height of 10 m. The first reason this turbine is chosen is the availability of the power characteristics. The power curve of this turbine (Figure 2.1) is derived from a field study by NREL (National Renewable Energy Laboratory) technical report [12] in accordance with international standards (IEC 61400-12-1) and field tests from Dabiri's paper [4]. In Appendix C, Table C.18, the turbine parameters are summarized.
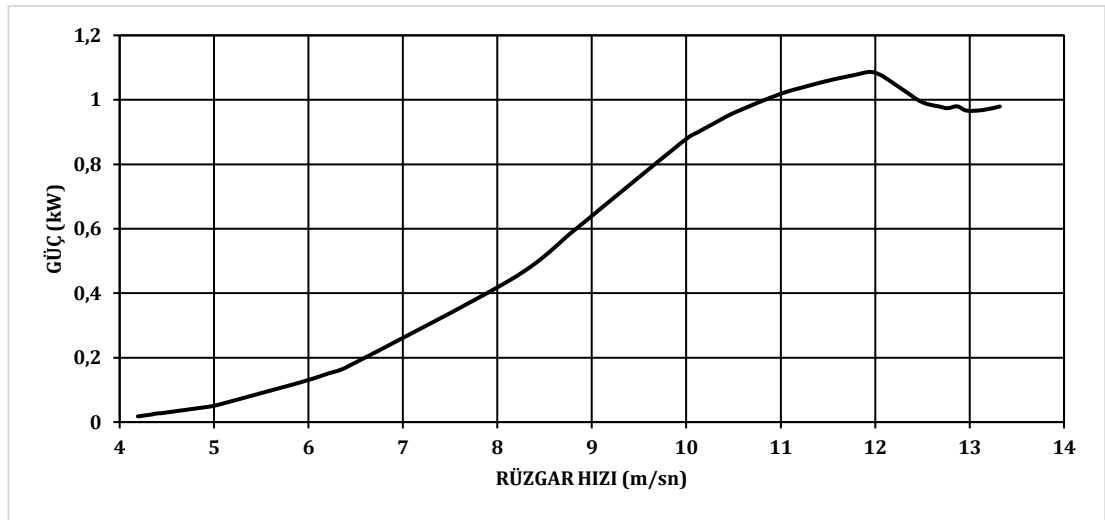
Figure 2.1 : Power curve of Mariah Windspire 1.2 kW.

2.2 Site Information

The site is located in the Çaltılıdere Town of northern Aliağa District, Izmir, Turkey. The site is completely open to the sea from the north and west. It has small hills and short vegetation. It has a ruggedness index of almost 0% and it is not very sloped. The site is located at an altitude of 70 m and has a prevailing wind direction (PWD) from the north-east (Figure 2.2). Since the site has mild slopes, small hills, and the presence of the shoreline places the site in the semi-complex class (Figure 2.3) (Figure 2.4) [13].

7
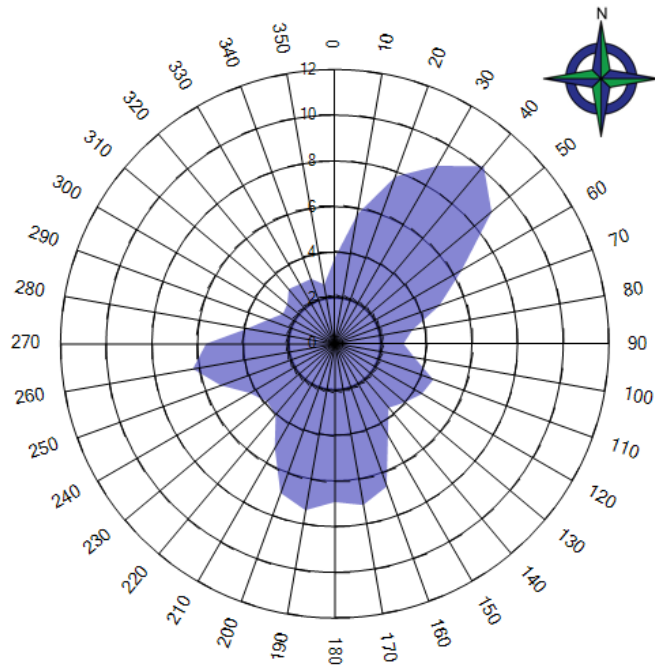
Figure 2.2 : Histogram of the measured wind direction.

Figure 2.3 : Aerial view of the site (38.862526 Latitude, 27.047738 Longtitude).

In figure 2.5, the power density of the area is given. Calculations are made in WAsP application. The power density where the turbine is sited is 219 W/m^2 for the sample turbine used in this study.
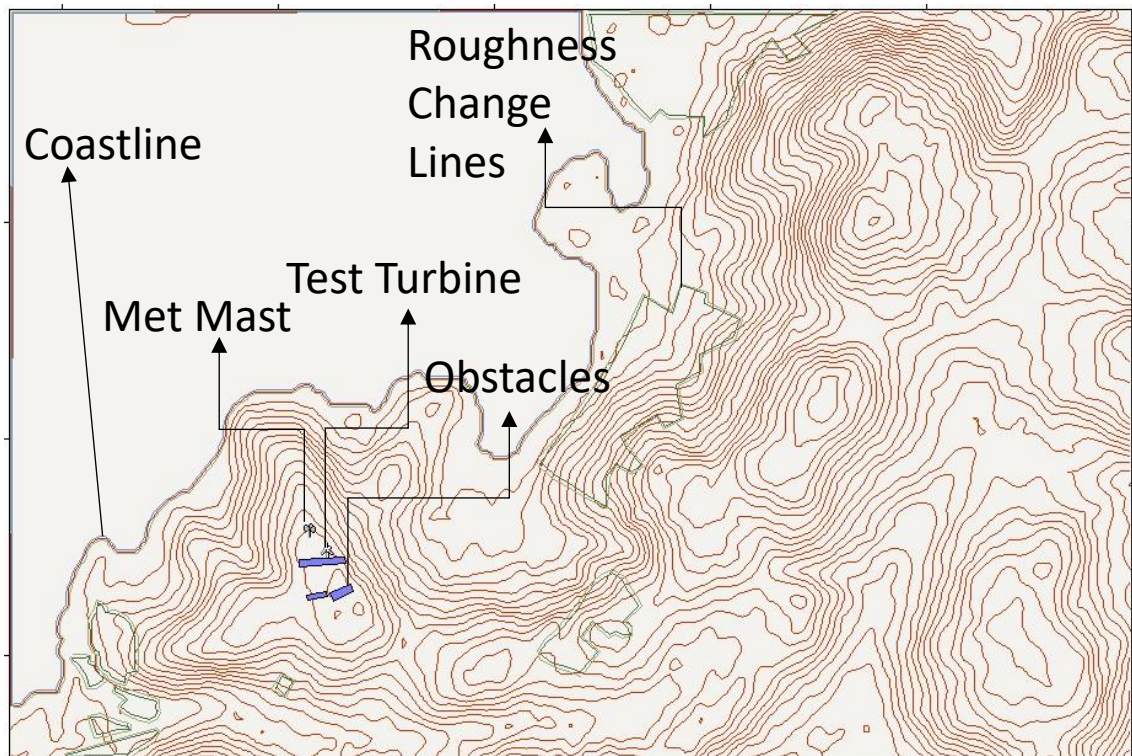
Figure 2.4 : Vector map of the test site (3 km x 2 km) with 5 m height contour distance and 1 arc second (30 m) resolution.
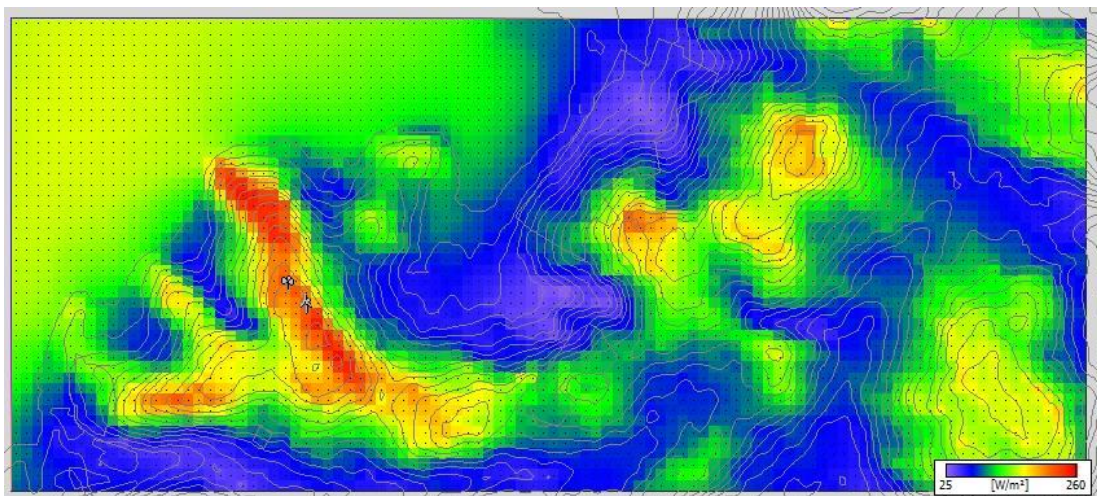
Figure 2.5 : Power density of the site with an average value of 113 W/m^2.

2.3 Measurement Data

In order to determine the wind characteristics of the site, wind direction and velocity data recorded for approximately 15 months between June 26, 2012 and November 1, 2013 (Figure 2.6). Measurements were made at the same point as the turbine position at 30, 58 and 60 m altitudes with 10-minute averages. Considering the available data within the scope of this study, it is anticipated that the use of data at 30 m, which is the closest elevation to the 8 m height (hub-height), will not lead to big differences in

terms of results and it is deemed appropriate to use this data since it is known that the software to be used (WAsP) can carry these values to 8 m height with certain statistical methods.
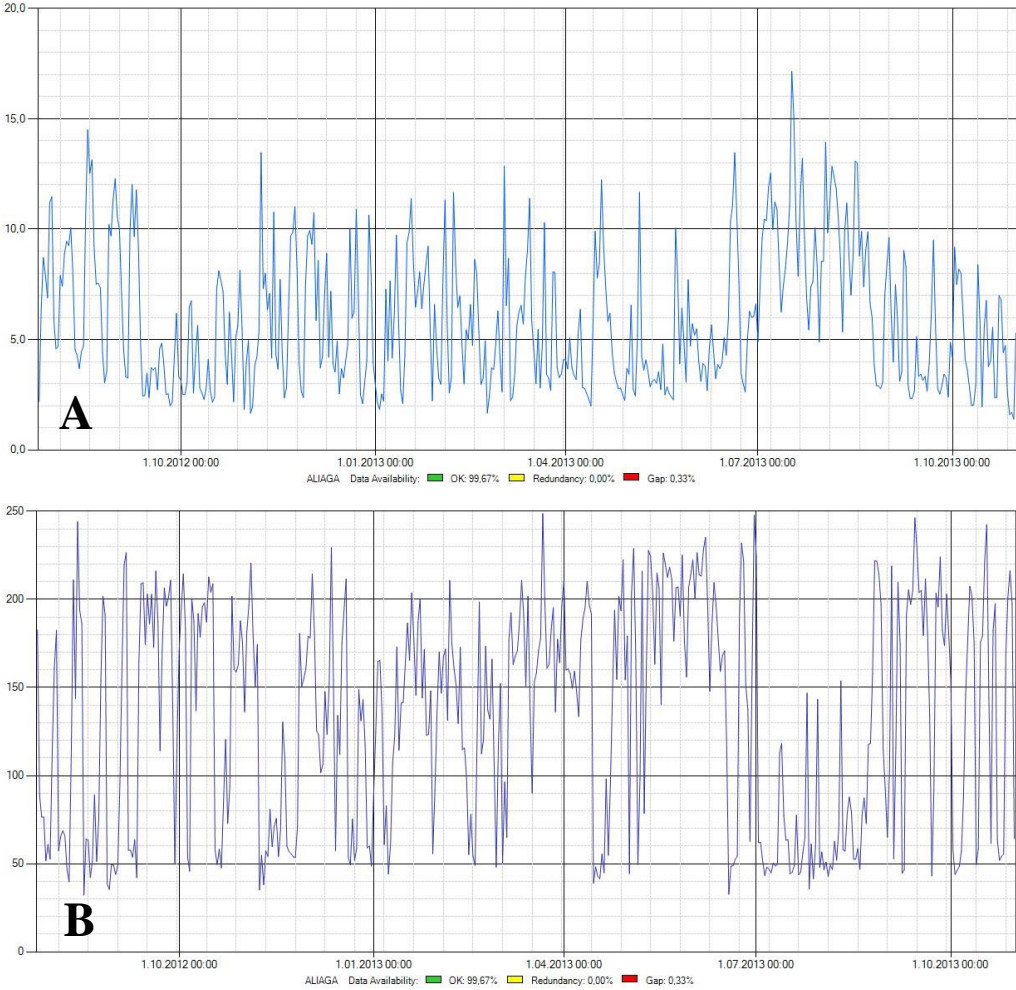
Figure 2.6 : Daily means of wind speed (A) and wind direction (B) measurements.

The anemometer and the windvane used in this study are Kintech Engineering, Thies First Class Advanced and THIES COMPACT TMR respectively. The anemometer has an accuracy of ±0.2 m/s and the windvane has an accuracy of ±2°. Data from the meteorological mast logged with Kintech Engineering, EOL Zenith Data Logger and transmitted with GSM cell modem.

2.4 Data Preparation

Nowadays, the software used in the annual power generation (AEP) calculations (e.g. WAsP and WindPRO) is designed for HAWTs. However, when certain parameters are considered, it can be seen that VAWTs can be examined with these software. WAsP,

which is the software used in this study, conducts the wake analysis in according to HAWTs. The thrust coefficient parameter is used to carry out the wake analysis. However, the analysis of the wake is important only if more than one turbine will be located on the site because this analysis is used to calculate the aerodynamic interactions between the turbines in the field. This study was carried out only for a pair of VAWT. Since these interactions between a pair of VAWT are known from the literature [4], this VAWT pair can be defined as a single turbine. Thus, the wake calculations of WAsP do not affect the result.

Since the wakes of wind turbines affect the performance of the turbines around them, the total annual energy production of the turbines becomes a function of the wind direction. For this reason, annual energy production of the turbines should be calculated by taking into consideration the change of wind direction during the year. There are no commercially available tools in the literature that can be used in this calculation. However, there are experimental and numerical studies examining the change in the total power coefficient (equivalent power coefficient of two turbines) of paired VAWTs according to wind direction [4;7;8]. The polar diagram taken from such a study [4] (Figure 2.7) was used as the main data source for the calculation of AEP of paired VAWTs in this study.
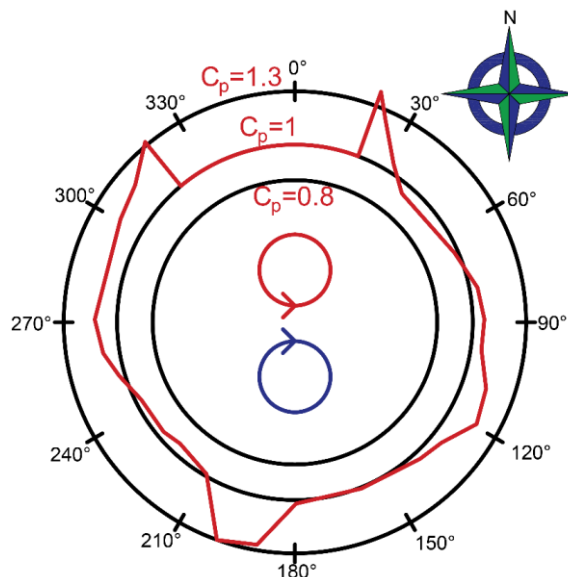
Figure 2.7 : Change of the power coefficient (radial coordinate, red line) normalized to the incoming wind direction (angular coordinate). Red and blue circles indicate turbines and the arrows indicate their rotational direction.

The ratio of the electrical power generated by the turbine and mechanical power of the undisturbed air stream is called the power coefficient [14]. The power coefficient is

$$C_p = \frac{P}{\left(\frac{1}{2}\right)\rho A U^3}$$

(2.1)

Here, P is the generated electrical power, ρ is air density, A is turbine rotor swept area, and U is the wind speed. A normalized power coefficient, C_p^{norm}, defined as the ratio of the turbine power coefficient in the coupled VAWT configuration to the power coefficient of the isolated turbine [4]. Then the coupled VAWT configuration's power coefficient becomes

$$C_p^{coupled} = C_p^{norm} \times C_p^{isolated}$$

(2.2)

2.5 Data Analysis

While analyzing the data, the diagram in Figure 2.7 is divided into sectors in order to examine the turbines' behavior related to the direction of the wind. n being the number of sectors, angular intervals ($\Delta\theta$) is determined by

$$\Delta\theta = \frac{360}{n}$$

(2.3)

After determining the sector number and angular intervals, the position of the sectors around the turbines should be determined. With respect to the north direction, in Figure 2.8-a, the locations of the sectors around the turbine pair are shown. Average C_p^{norm} value for each $\Delta\theta_i$ sector to be $\overline{C_{p,\iota}}$ and the number of C_p^{norm} data for the sector to be m, $\overline{C_{p,\iota}}$ value can be determined by

$$\overline{C_{p,\iota}} = \frac{\sum_{j=1}^{m} C_{p,j}^{norm}}{m}$$

(2.4)

In all calculations, the $\overline{C_{p,\iota}}$ value is considered constant for each individual sector.

In Figure 2.8-b, the variation of the $\overline{C_{p,\iota}}$ value for the n = 6 condition is shown graphically. By increasing the number of sectors (n), the angular resolution and the accuracy of the analysis can be increased.

The sectors where the turbines have a maximum and minimum performance can be used to determine the positions of the angular intervals. For example, during this

positioning, where the turbines perform their maximum performance (e.g. Figure 2.8-b, 150°-210°) and where the maximum potential of the site is located (PWD) (Figure 2.2, 15°-75°) superposed, $\overline{C_{p,\iota}}$ values are also exchanged every other sector and as a result, the effect of the wind coming from all directions to the turbine pair for each turbine layout must be calculated separately. Therefore, the calculated $\overline{C_{p,\iota}}$ values are multiplied by the power production values of the isolated turbine and a new turbine power curve is defined in each individual sector.
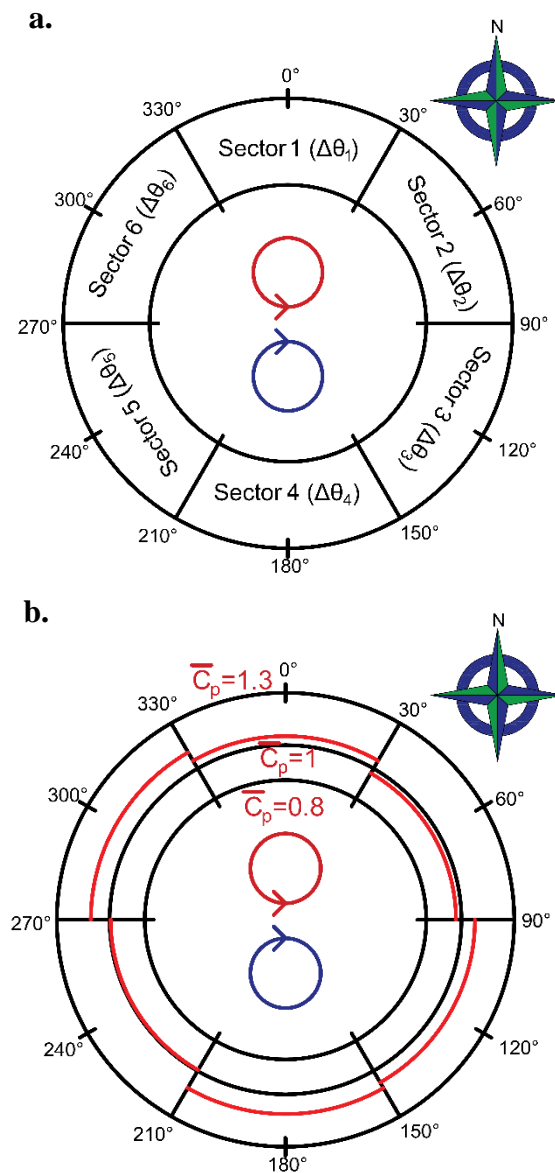
Figure 2.8 : Sample graphical representation of sectors (a) and calculated $\overline{C_{p,\iota}}$ values (red lines) (b).

While WAsP calculates the AEP, it considers the turbines in the field as HAWTs and this leads to the inclusion of the winds coming from all directions to the calculation. This can be included to the calculation under real conditions by means of the yaw mechanism in HAWTs. In order to adapt this calculation to the coupled VAWT pair, the wind coming from all directions must be separated into sectors (Δβi) and analyzed with the power curve in its own sector. The value of the AEP that WAsP finds for each individual sector is multiplied by a coefficient found by the ratio of the number of wind frequency (Δβi) (Figure 2.9) found in that sector only to the total number of wind frequency (Δβ$_{total}$) in order to find the real AEP value for an individual sector

$$AEP_{WAsP,i} \times \frac{\Delta\beta_i}{\Delta\beta_{total}} = AEP_{\Delta\theta_i} \tag{2.5}$$

Then the total real AEP value found by summation of AEPs for all individual sectors

$$\sum_{i=1}^{n} AEP_{\Delta\theta_i} = AEP_{Real} \tag{2.6}$$

The work flow diagram of the method is shown in Figure 2.10.
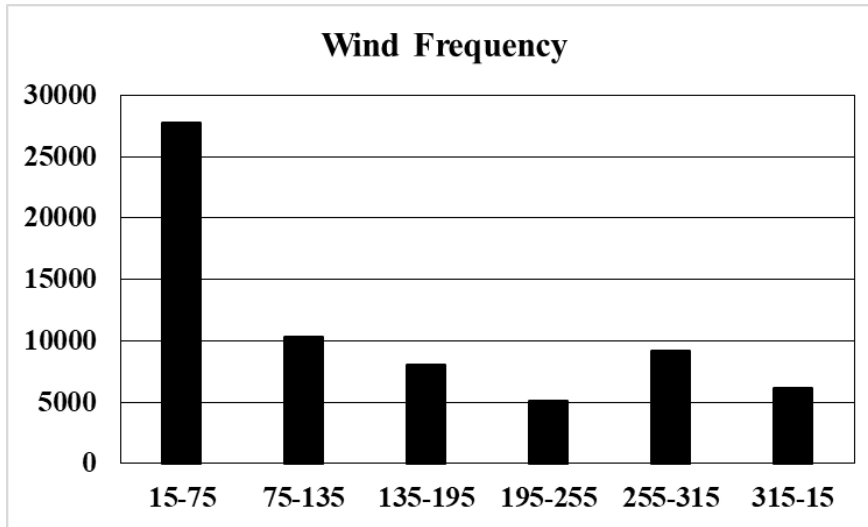
Figure 2.9 : Number of wind frequency by sectors. PWD is between 15°-75°.

$$C_p^{normalize}(\theta)$$

$\downarrow$

Dividing into sectors
$$360 \div n = \Delta\theta_i$$

$\downarrow$

Evaluation of average $C_p^{normalize}(\theta)$
$$\bar{C}_p(\Delta\theta_i)$$

$\downarrow$

Creating new turbine power curves
by multiplying $\bar{C}_p(\Delta\theta_i)$ by isolated turbine's
power generation values

$\downarrow$

Dividing the wind data
into sectors ($\Delta\beta_i$)

$\downarrow$

Inserting the wind and turbine data
to WAsP as inputs, sector-wise
And executing analyses

$\downarrow$

Multiplication of calculated AEP values by the ratio of
wind frequency of the individual sector
to the total wind frequency
$$AEP_{WAsP} \times \frac{\Delta\beta_i}{\Delta\beta_{total}} = AEP_{\Delta\theta_i}$$

$\downarrow$

Summation of AEP values
for each individual sector
$$\sum_{i=1}^{n} AEP_{\Delta\theta_i} = AEP_{Real}$$

Figure 2.10 : Work flow diagram of the method.

3. RESULTS AND DISCUSSION

3.1 Sample Application

In order to apply the proposed method to the site using the sample turbine type, the power coefficient line (red line) indicated by polar coordinates in the diagram in Figure 2.7 is divided into six 60° angular intervals in the sectors where turbines are expected to perform differently. The turbine data and the field data match is visualized in Figure 3.1 by combining the calculated $\overline{C_{p,\iota}}$ values and the wind direction distribution data (Figure 2.2) for these regions. The two separate turbine siting shown in Figure 3.1 indicate that an optimization solution must be made in which the direction-dependent change in the performance of the turbine pair is combined with the field data in order to maximize the value of the AEP.

In order to demonstrate the variation of the performance of the turbine pair in the field, for example, five regions in which the turbines may perform well or poorly are selected. These are:

    a) Between 30°-90° (bad performance)

    b) Between 90°-150° (mediocre performance)

    c) Between 150°-210° (good performance)

    d) Between 210°-270° (bad performance)

    e) Between 260°-320° (best performance)

When selecting these regions, the sequence of 260°-320° instead of 270°-330° is selected specifically because this angle range is the 60° interval with the highest $\overline{C_p}$ value.

In order to evaluate the different possibilities that may occur in the siting of the turbine pair, a comparison is made for different situations where these regions are placed in such a way that the desired sector faces the PWD (15°-75°). The configurations that are calculated are shown in Figure 3.2.
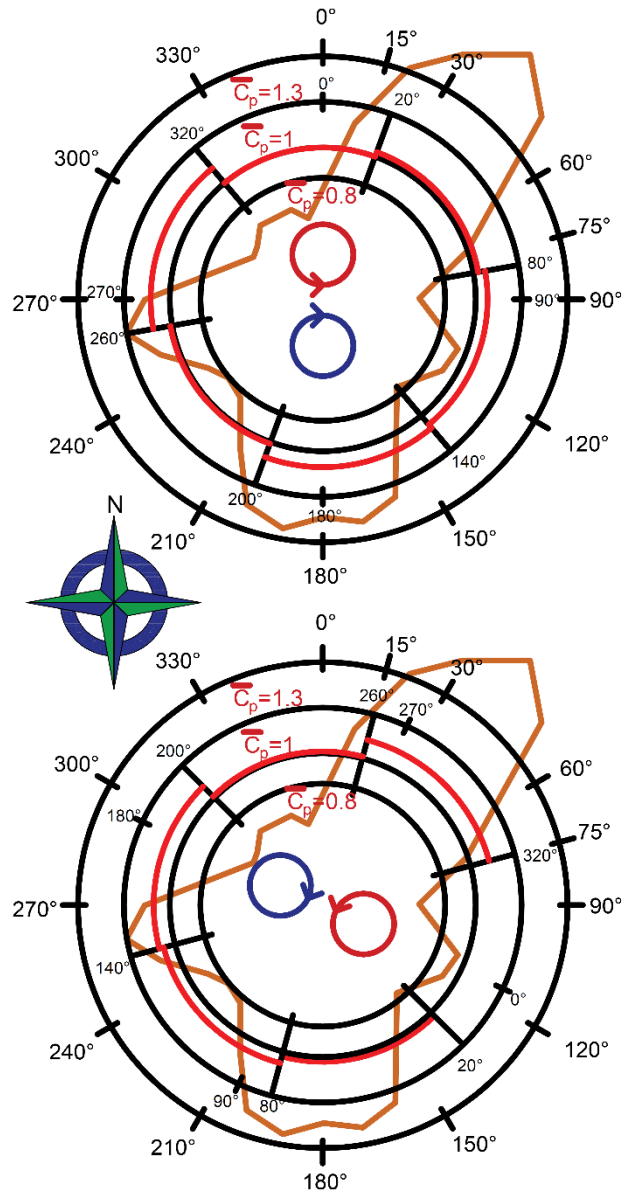
Figure 3.1 : A sample representation of the rotation of the power coefficient line and the turbines. Brown line shows the wind direction distribution while the red lines are $\overline{C_{p,\iota}}$.

As an example, while creating the 260°-320° placement which has the highest $\overline{C_p}$ value (Figure 3.2-e), while 260°-320° sector rotates to face the PWD, the remaining sectors are also rotate together. The result of these different configurations was compared with the performance of two VAWTs, which were located in the same position on the site and were isolated from each other.
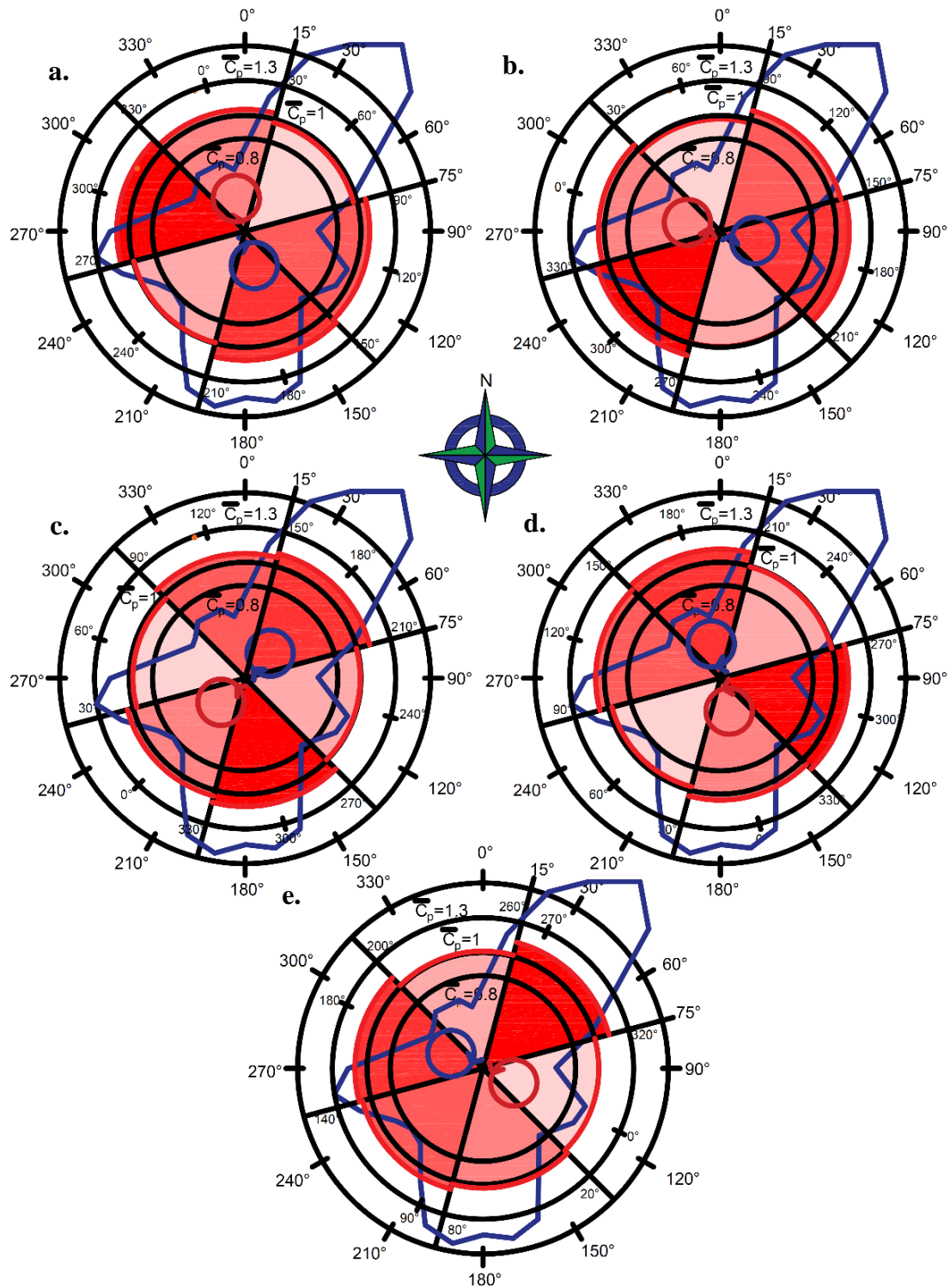
Figure 3.2 : Schematic representation of different angular positions relative to sectors. (The $\overline{C_p}$ value increases as the color darkens.) (a: 30°-90°, b: 90°-150°, c: 150°-210°, d: 210°-270°, e: 260°-320°)

In order to distinguish the turbines' response in different sectors, the $\overline{C_p}$ values corresponding to the angular intervals were multiplied by the power generation values of the isolated turbine (Appendix D, Table D.19). The turbine power curves used for

each 60° angular interval are given in Appendix B, Table B.16 and Table B.17. In Figure 3.3, a sample representation of the power curve is shown.
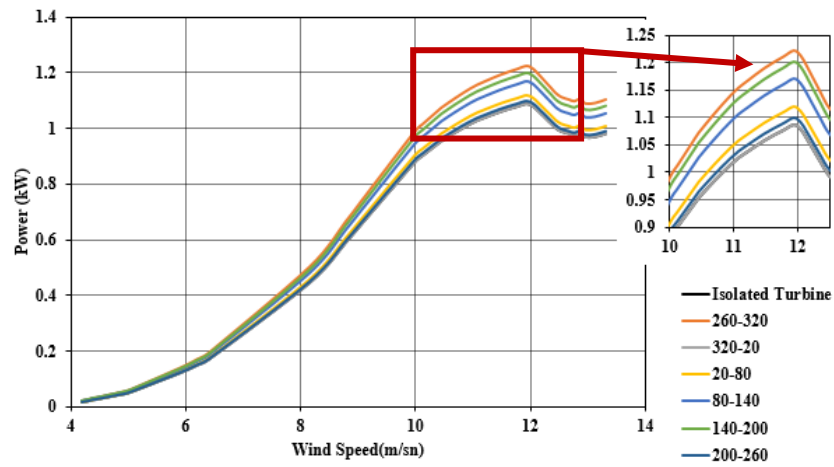
Figure 3.3 : A sample representation of power curve variations of the 260°-320° configuration by sector. (Black line and gray line overlapped as the power curve representing the 320°-20° equals to the power curve of the isolated turbine.)

3.1.1 Effect of resolution change

As mentioned above at Section 2.5, increasing the number of sectors, *n,* affects the AEP output of configurations. In this study, 15° and 30° intervals are also examined in addition to the 60° intervals. Increasing the number of sectors from *n=6 to n=12* and *n=24* gives 30° and 15° angular intervals respectively. Applying the method described above, analyses were done to investigate the effect of resolution change. The average normalized power coefficient and wind data are separated and calculated for each individual angular interval. For example, when the resolution is changed to 30°, 30°-90° configuration is also separated into two intervals; 30°-60° and 60°-90°. For the sake of simplicity, these configuration names are kept the same in the figures and tables given in this chapter. All the data used in the analyses and corresponding AEP values are given in Appendix A, Table A.1-15.

Figure 3.4 shows the effect of resolution change graphically. In this figure, each configuration in each resolution is shown by the same color. Slight changes at AEPs were observed as a result of these analyses. Since the power coefficient data is sliced into smaller intervals, it becomes better and easier to get an understanding of the AEP in a specific sector. It can be seen that as the resolution increases, the contribution of each angular interval to the total AEP can be understood more clearly.
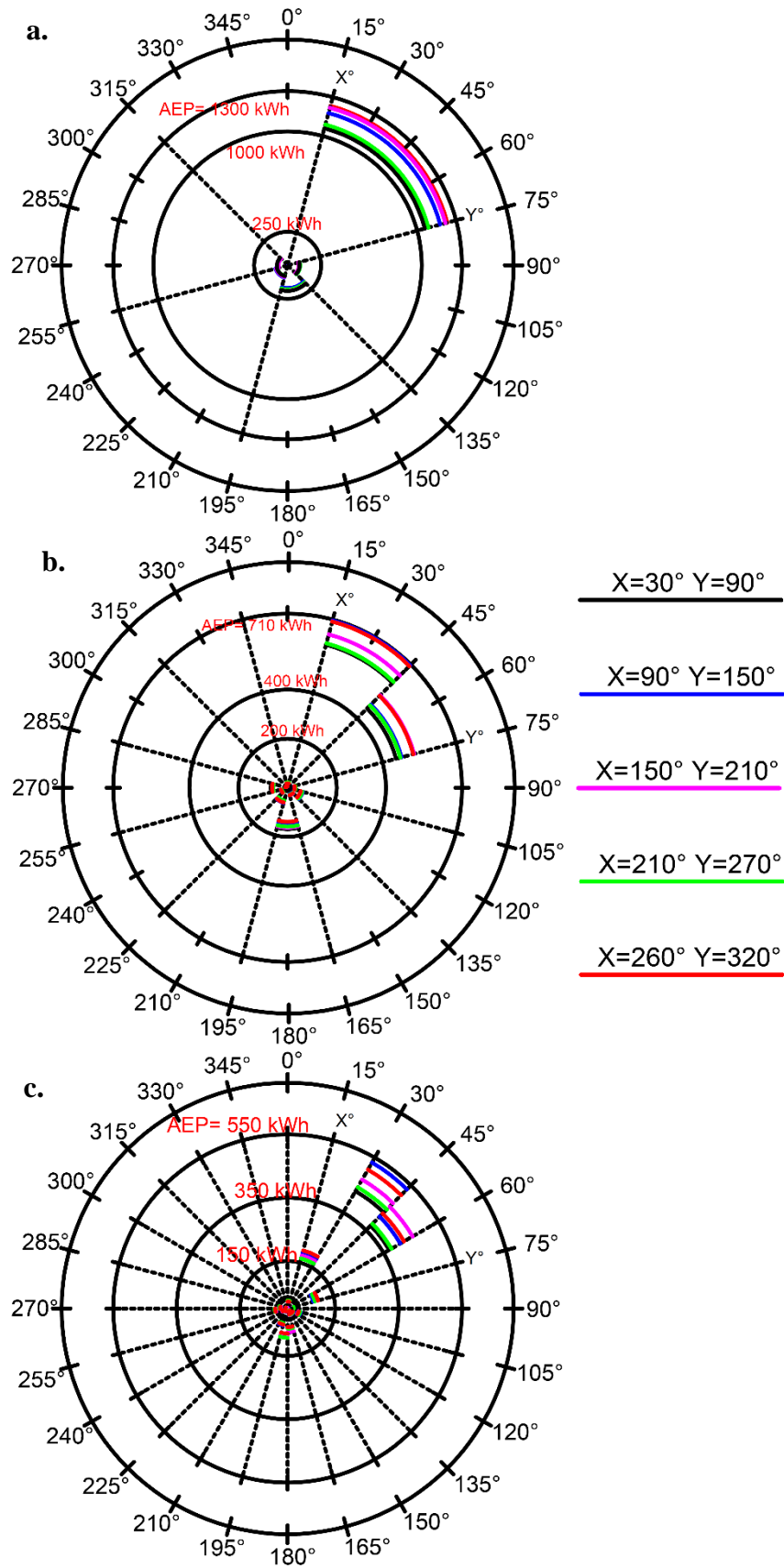
Figure 3.4 : Representation of AEP values sector by sector.(a: 60 degree intervals, b: 30 degree intervals, c: 15 degree intervals)

It should be noted that wind frequency plays an important role at AEP. Figure 3.4-c shows that between 15 and 75 degrees, 30°-60° angular interval contributes more to the AEP since the wind frequency here is the most. The rest has very small contributions to the AEP.

In Figure 3.4-a, the 260°-320° configuration shows the best performance between 15°-75°. However, when we increase the resolution to 30 degree interval (Figure 3.4-b) it can be seen that between 15°-45°, 90°-150° configuration performs slightly better. Further increase of resolution to 15° shows the AEP contributions clearer and the superiority of the 90°-150° configuration over 260°-320° configuration between 30°-45°. This is because of the separation of the power coefficient and wind data used in this study. Between 30°-45°, the $\overline{C_p}$ value of 90°-150° configuration is greater than the $\overline{C_p}$ value of 260°-320° configuration and with the use of the same wind data between this angular interval, 90°-150° configuration performed better AEP-wise.

Since the chosen PWD is between 15°-75° in this study, Figure 3.4-c shows that, the contribution to the AEP between 15°-30° and 60°-75° is much less than between 30°-60° interval. This also means the wind frequency data should be investigated more detailed for further research. The other angular intervals contributed much more less since the wind dominantly comes through 15°-75°.

3.2 Results and Comparison

AEP values and performance enhancements are summarized and compared with the isolated turbine pair in Table 3.1-3.

Table 3. 1 : Performance enhancements of coupled VAWT pair configurations' AEPs compared to AEP of isolated VAWT pair (60-degree intervals).

CONFIGURATION	AEP (kWh)	PERFORMANCE ENHANCEMENT	CAPACITY FACTOR
Isolated	2990	-	28.4%
30-90	3058.891	2.25%	29.10%
90-150	3267.087	8.48%	31.08%
150-210	3349.264	10.73%	31.86%
210-270	3091.949	3.30%	29.41%
260-320	3373.691	11.37%	32.09%

Table 3. 2 : Performance enhancements of coupled VAWT pair configurations' AEPs compared to AEP of isolated VAWT pair (30-degree intervals).

CONFIGURATION	AEP (kWh)	PERFORMANCE ENHANCEMENT	CAPACITY FACTOR
Isolated	2990	-	28.4%
30-90	3071.458	2.65%	29.22%
90-150	3294.629	9.25%	31.34%
150-210	3277.966	8.78%	31.18%
210-270	3102.578	3.63%	29.51%
260-320	3347.672	10.68%	31.85%

Table 3. 3 : Performance enhancements of coupled VAWT pair configurations' AEPs compared to AEP of isolated VAWT pair (15-degree intervals).

CONFIGURATION	AEP (kWh)	PERFORMANCE ENHANCEMENT	CAPACITY FACTOR
Isolated	2990	-	28.4%
30-90	3054.112	2.10%	29.05%
90-150	3345.916	10.64%	31.83%
150-210	3308.766	9.63%	31.48%
210-270	3089.207	3.21%	29.39%
260-320	3320.518	9.95%	31.59%

Figure 3.5 shows the comparison of the AEP with the change of resolution. Chosen sectors and the resolution method performed as predicted since WAsP uses statistical methods to calculate the AEP. However, slight movements at the AEP with the resolution change followed a mixed order, meaning; this method needs to be researched more elaborately in order to find the best method to discover the most efficient configuration.
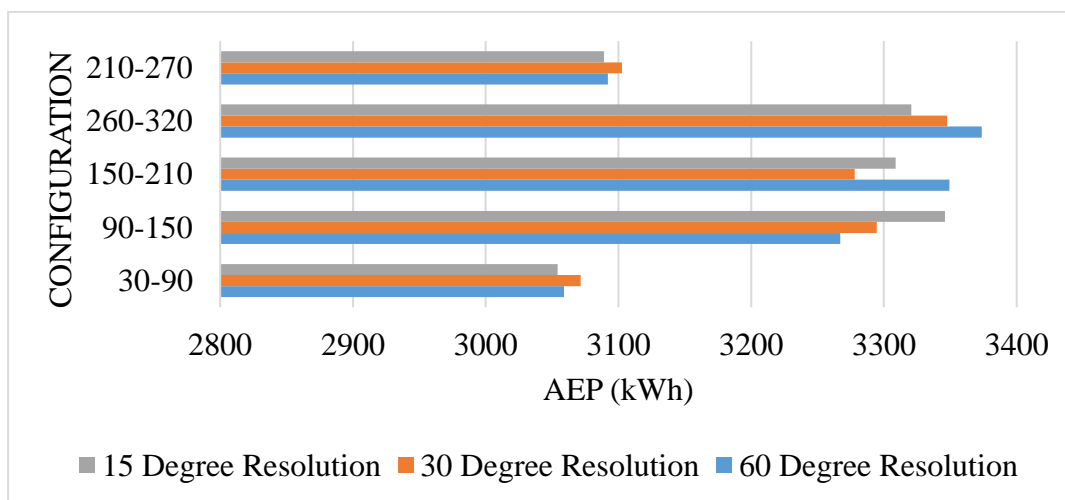
Figure 3.5 : Change of AEP by configurations and resolutions.

The 15 degree resolution considered to be the most accurate resolution method since the data used is sliced into smaller parts and analyzed more detaily. Regarding this, there are overestimates and underestimates appearing in this method. In this study, these over and underestimations fluctuate $\pm 2\%$. Considering the site and turbine specifications used in this study, these fluctuations may appear greater than $\pm 2\%$ when a large scale turbine and a completely different site are used. This also leaves an open door for a further research.

The comparison of the configurations should also be discussed. Placement of the turbines also creates a great difference while calculating the AEP. Between the worst and best performances there is approximately 10% difference for AEP considering the data used in this study (Figure 2.7). When other types of VAWTs are used, this deviation may differ according to their blade shapes, generator power or height etc. Also the spacing between paired turbines has an impact on energy production. In Dabiri's work [4], this spacing is kept constant at 1.65 diameter. There are also other studies researching the performance difference that the spacing between paired VAWTs create [8;16;18;19;20]. Method used in this study also can be implemented to this situation for further research.

3.3 Sensitivity Analysis

3.3.1 Obstacle sensitivity

The porosity is the ratio of the area of the windbreaks 'pores', to its total area and as a general rule, the porosity can be set equal to zero for buildings and 0.5 for trees. A row of similar buildings with a separation between them of one third the length of a building will have a porosity of about 0.33, as mentioned in WAsP help files. The lesser the value the more dense the obstacle. Porosity values of obstacles set to values of 0, 0.5 and 1 in order to investigate the effect of obstacles while calculating the AEP. As a result, no considerable changes observed. A minor AEP change of ± 2 kWh considered negligible.

3.3.2 Turbulence intensity

The uncertainty of turbulence effects should also be considered. The same method was used to study the effects of the turbulence intensity while calculating the AEP. Turbulence intensity (TI) basically can be expressed as

$$TI = \frac{\sigma}{U_{avg}} \tag{3.1}$$

Here, σ is the standard deviation and U_{avg} is the mean wind speed.

The data series used to calculate AEP in this study also contains 10 minute averaged intervals of standard deviations for each corresponding 10 minute averaged wind speed. With this data, turbulence intensity of each 10 minute interval was calculated and average turbulence intensity of the site was found 17% with an arithmetic average. n being the number of data, average TI can be found by

$$TI_{avg} = \frac{\sum_{i=1}^{n} \frac{\sigma_i}{U_i}}{n} \tag{3.2}$$

After that, 10 minute intervals which has TI above %17 percent was removed from the data series in order to get a smoother Weibull distribution. Using the same method calculations were taken place. A great increase of AEP was observed by 488 kWh for one turbine in the isolated pair. However, the enhancements were almost stayed the same. Table 3.4 shows the AEP calculations of turbulence intensity sensitivity analysis for every configuration with 60 degree intervals.

Table 3. 4 : Turbulence intensity sensitivity analysis results.

CONFIGURATION	AEP (kWh)	PERFORMANCE ENHANCEMENT	CAPACITY FACTOR
Isolated	3966	-	37,73%
30-90	4039,23	1,81%	38,42%
90-150	4326,67	8,34%	41,16%
150-210	4431,13	10,50%	42,15%
210-270	4087,39	2,97%	38,88%
260-320	4470,81	11,29%	42,53%

As it can be seen in Figure 3.6, after removing the data, which has above average turbulence intensity at the site, the AEP values increased by approximately 1 MWh in each VAWT pair configuration. Turbulence intensity is higher when the wind speed is lower and the standard deviation is higher. Removing the low wind speeds from the data series made the site more efficient and increased the AEP.

The topographical conditions of the site has a big impact on the turbulence intensity. The effect of topographical slope angle were investigated by Park M. and Park S. [17]. It is found that sloping terrain enhances the turbulence intensity compared to flat surface. Since the test site used in this study is over a hill with a slightly sloped terrain,

it can be anticipated that the turbulence intensity may be an issue while calculating the AEP. This also creates an another topic for further research.
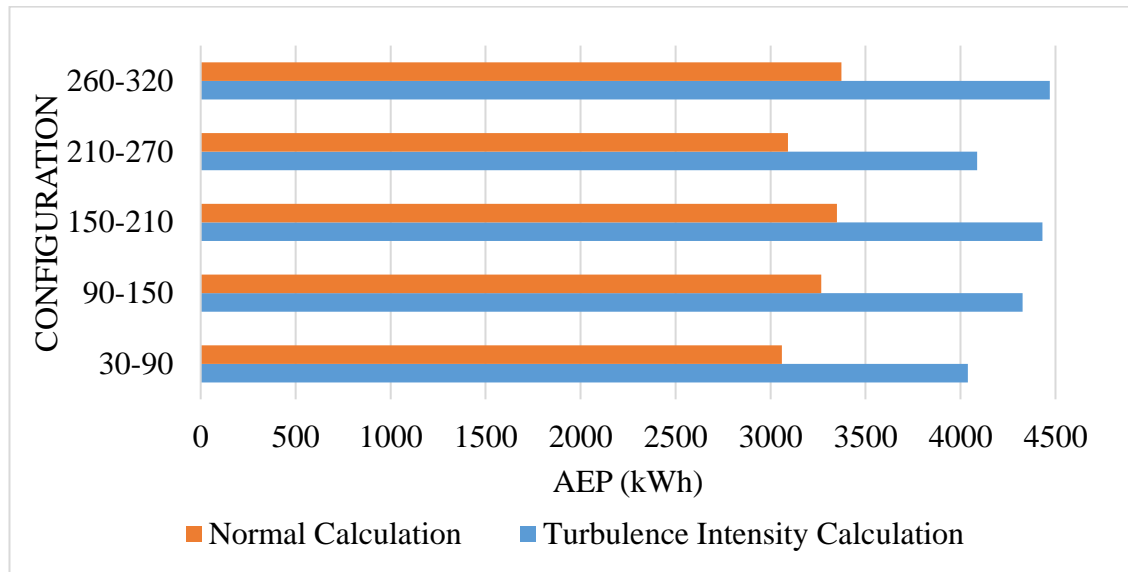
Figure 3.6 : Comparison of normal and turbulence intensity sensitivity calculation.

3.3.3 Altitude sensitivity

In order to test the WAsP's extrapolation of wind data, the hub-height of the turbine increased from 8-m to 30-m to calculate the AEP. The calculations were resulted with an increase of AEP by 543 kWh, from 1495 kWh to 2038 kWh. Meaning, WAsP's extrapolation algorithm works under 10-m altitude but the accuracy of it still needs to be investigated more detaily.

3.3.4 Additional uncertainties

When the calculations were made, the air density value of the field, which has 70 m altitude and an average air temperature was 18°C in the year, was taken as 1.2 kg/m^3 and the uncertainties due to the deviations seen during this year were not taken into consideration.

The resolution of the vector map used is also of great importance when making calculations. In this study, topographic map with 1 arc-second resolution was used. The projections of the vector map and the spatial image of the area were taken from platforms that uses WGS84 projection system. However, when both maps are overlapped there is a slight misalignment. This is because the projection system of spatial image which is EPSG 3857, uses a coordinate system projected from the surface

of the sphere or ellipsoid to a flat surface, meaning; EPSG 3857 uses a coordinate system the same as a map (flat surface). Whereas, the projection system of the vector map is EPSG 4326 which uses a coordinate system on the surface of a sphere or ellipsoid of reference, so, it uses a coordinate system the same as a globe (curved surface). As a result, the more you move away from the equator the more elongated the map will be. This will cause roughness change lines, obstacles and other important locations to be misaligned on the map. Since this study uses a very small portion of the map compared to the whole of the map, these effects were considered negligible.

There may be deviations in the results because the working turbine data is taken from a flat field. It is also important to examine how the proposed method is affected from the field conditions (roughness, orography, obstacles) and to correct the method according to the field conditions. All these fields of study are thought to be an opportunity for researchers and commercial institutions.

Due to the different working patterns and aerodynamic interactions, it is necessary to develop new approaches for VAWTs and coupled VAWTs for AEP estimations. In this study, a method that can be used for the calculation of AEP of a single pair of coupled VAWT is proposed.

4. CONCLUSION

As the result of the analyses, two isolated VAWTs were found to have a total AEP of 2990 kWh. Even in the worst-case scenario, paired VAWTs performed better than the isolated ones, showing AEP enhancement of %2.25 and furthermore they showed a performance increase of over 10% for different configurations (Table 3.1-3). When the ratio of the turbine's annual average power production to the turbine's rated power evaluated, which is the capacity factor [15], the commercial performance of the turbines in the field can be understood more clearly. Table 3.1-3 shows the capacity factor of different configurations.

In the sample application, it was shown how important siting in the field was examined and it was shown that the performance could be increased by up to 10% with correct siting. There are some uncertainties as the calculation software used is developed for HAWTs. As a result of this, the examination of the errors that may occur would improve the method.

A performance increase of approximately 10% in a single pair is very satisfying both for commercial and technical view. By increasing the number of sectors (n) furthermore, the angular spacing ($\Delta\theta$) can be reduced to increase the angular resolution and improve the accuracy of the analysis.

It is known from the experimental research of Dabiri [4], VAWTs are greatly better than HAWTs considering power density per floor-area when they are paired. Currently used HAWT farms can be upgraded using VAWTs, setting out the VAWTs on HAWT farms like a bush-tree concept, making the wind farms much more efficient areawise.

REFERENCES

[1] BP Statistical Review of Wold Energy, 67th Edition (June 2018)

[2] World Wind Energy Association - Statistics, https://wwindea.org/information-2/information/

[3] Karadeniz, Z. H. (2015). Düşey eksenli rüzgar türbini araştırmalarında son gelişmeler, *VIII. Yenilenebilir Enerji Kaynakları Sempozyumu*, 15-16 October, Adana, Turkey, 151-155.

[4] Dabiri, J. (2011). Potential order-of-magnitude enhancement of wind farm power density via counterrotating vertical-axis wind turbine arrays. *Journal Of Renewable And Sustainable Energy, 3*(4). doi: http://dx.doi.org/10.1063/1.3608170

[5] Iida, A., Mizuno, A. & Fukudome, K. (2007). Numerical simulation of unsteady flow and aerodynamic performance of vertical axis wind turbines with LES, *16th Australasian Fluid Mechanics Conference*, 2-7 December, Crown Plaza, Gold Coast, Australia, 1295-1298

[6] Mertens, S., Van Kuik, G. & Van Brussel, G. J. W. (2003). Performance of a high tip speed ratio H-Darrieus in the skewed flow on a roof, *41st Aerospace Sciences Meeting and Exhibit*, Reno, Nevada, USA, Paper No. AIAA-2003–0523

[7] Whittlesey, R. W., Liska, S. & Dabiri, J. (2010). Fish schooling as a basis for vertical axis wind turbine farm design, *Bioinspiration & Biomimetics*, *5*, 1-6. doi: http://dx.doi.org/10.1088/1748-3182/5/3/035005

[8] Zanforlin, S. & Nishino, T. (2016). Fluid dynamic mechanisms of enhanced power generation by closely spaced vertical axis wind turbines. *Renewable Energy, 99,* 1213-1226. doi: http://dx.doi.org/10.1016/j.renene.2016.08.015

[9] Bowen, A. J. & Mortensen, N. G. (2004). WAsP prediction errors due to site orography. Denmark. Forskningscenter Risoe. Risoe-R, No. 995(EN)

[10] Troen, L. & Petersen, E. L. (1989). European Wind Atlas, Riso National Laboratory

[11] Jae-kyoon, W., Hyeon-gi, K., Byeong-min, K., In-su, P. & Neung-soo, Y. (2012). AEP prediction of a wind farm in complex terrain - WindPRO vs. WindSim, *Journal of the Korean Solar Energy Society, 32*(6), DOI: 10.7836/kses.2012.32.6.001

[12] Huskey, A., Bowen, A. & Jager, D. (2009). Wind turbine generator system power performance test report for the Mariah Windspire 1-kW wind turbine. *National Renewable Energy Laboratory Technical Report,* Project Number: NREL/TP-500-46192

[13] Bingöl, F. (2010). Complex terrain and wind lidars (Doctoral dissertation). Roskilde: Risø National Laboratory for Sustainable Energy. Risø-PhD, No. 52(EN)

[14] Hau, E. (2005). Wind Turbines: Fundamentals, Technologies, Application, Economics. Berlin: Springer

[15] Albadi, M. H. & El-Saadany, E. F. (2009). Wind turbines capacity factor modeling—A novel approach. *IEEE Transactions On Power Systems*, *24*, 1637-1638. doi: http://dx.doi.org/10.1109/TPWRS.2009.2023274

[16] Kinzel, M., Mulligan, Q. & Dabiri J. (2012). Energy exchange in an array of vertical-axis wind turbines. *Journal of Turbulence, 13*(38), 1-13. doi: http://dx.doi.org/10.1080/14685248.2012.712698

[17] Park, M. & Park, S. (2006). Effects of topographical slope angle and atmospheric stratification on surface-layer turbulence. *Boundary-Layer Meteorology*, *118*, 613–633. doi: http://dx.doi.org/10.1007/s10546-005-7206-x

[18] Shaheen, M., El-Sayed, M. & Abdallah S. (2015). numerical study of two-bucket Savonius wind turbine cluster. *Journal of Wind Engineering and Industrial Aerodynamics, 137,* 78-89. doi: http://dx.doi.org/10.1016/j.jweia.2014.12.002

[19] Zuo, W., Wang, X. & Kang, S. (2016). Numerical simulations on the wake effect of H-type vertical axis wind turbines. *Energy, 106,* 691–700. doi: https://doi.org/10.1016/j.energy.2016.02.127

[20] Hezaveh, S. H., Bou-Zeid, E., Dabiri, J., Kinzel, M., Cortina, G., & Martinelli, L. (2018). Increasing the power production of vertical-axis wind-turbine farms using synergistic clustering. *Boundary-Layer Meteorology, 169(2), 275–296.* doi: https://doi.org/10.1007/s10546-018-0368-0

APPENDIX

APPENDIX A

Data gathered from the met. mast and WAsP software are given below in Table A.1-15. These data belong to one turbine in each pair. Multiplying by two gives the two turbines' total AEP.

Table A. 1 : Data used to calculate the AEP of 30°-90° configuration.

Config. Direction	Wind Direction	10 Minute Data Count Overall (Wind Frequency)	10 minute data count for wind direction	Ratio	AEP [kWh]	AEP Induced [kWh]
30-90	15-75	66488	27812	0.4183	2534	1059.974
90-150	75-135	66488	10289	0.1547	585	90.528
150-210	135-195	66488	8013	0.1205	1587	191.262
210-270	195-255	66488	5074	0.0763	1096	83.640
270-330	255-315	66488	9146	0.1375	576	79.233
330-30	315-15	66488	6154	0.0925	268	24.805
AEP for an isolated turbine [kWh] and all directions accounted for	1495		Total AEP Induced [kWh]		1529.445554	

Table A. 2 : Data used to calculate the AEP of 90°-150° configuration.

Config. Direction	Wind Direction	10 Minute Data Count Overall (Wind Frequency)	10 minute data count for wind direction	Ratio	AEP [kWh]	AEP Induced [kWh]
90-150	15-75	66488	27812	0.418301	2816	1177.936
150-210	75-135	66488	10289	0.15475	605	93.62359
210-270	135-195	66488	8013	0.120518	1417	170.774
270-330	195-255	66488	5074	0.076315	1220	93.10372
330-30	255-315	66488	9146	0.137559	547	75.24459
30-90	315-15	66488	6154	0.092558	247	22.86184
AEP for an isolated turbine [kWh]	1495		Total AEP Induced [kWh]		1633.543466	

Table A. 3 : Data used to calculate the AEP of 150°-210° configuration.

Config. Direction	Wind Direction	10 Minute Data Count Overall (Wind Frequency)	10 minute data count for wind direction	Ratio	AEP [kWh]	AEP Induced [kWh]
150-210	15-75	66488	27812	0.418301	2911	1217.674
210-270	75-135	66488	10289	0.15475	540	83.56485
270-330	135-195	66488	8013	0.120518	1578	190.1774
330-30	195-255	66488	5074	0.076315	1160	88.52485
30-90	255-315	66488	9146	0.137559	504	69.32956
90-150	315-15	66488	6154	0.092558	274	25.36091
AEP for an isolated turbine [kWh] and all directions accounted for		1495	**Total AEP Induced [kWh]**		1674.631904	

Table A. 4 : Data used to calculate the AEP of 210°-270° configuration.

Config. Direction	Wind Direction	10 Minute Data Count Overall (Wind Frequency)	10 minute data count for wind direction	Ratio	AEP [kWh]	AEP Induced [kWh]
210-270	15-75	66488	27812	0.418301	2600	1087.583
270-330	75-135	66488	10289	0.15475	601	93.00459
330-30	135-195	66488	8013	0.120518	1499	180.6565
30-90	195-255	66488	5074	0.076315	1068	81.50391
90-150	255-315	66488	9146	0.137559	560	77.03285
150-210	315-15	66488	6154	0.092558	283	26.19393
AEP for an isolated turbine [kWh] and all directions accounted for		1495	**Total AEP Induced [kWh]**		1545.974462	

Table A. 5 : Data used to calculate the AEP of 260°-320° configuration.

Config. Direction	Wind Direction	10 Minute Data Count Overall (Wind Frequency)	10 minute data count for wind direction	Ratio	AEP [kWh]	AEP Induced [kWh]
260-320	15-75	66488	27812	0.418301	2945	1231.897
320-20	75-135	66488	10289	0.15475	543	84.0291
20-80	135-195	66488	8013	0.120518	1471	177.282
80-140	195-255	66488	5074	0.076315	1188	90.66165
140-200	255-315	66488	9146	0.137559	575	79.09623
200-260	315-15	66488	6154	0.092558	258	23.87998
AEP for an isolated turbine [kWh]		1495	**Total AEP Induced [kWh]**		1686.845506	

Table A. 6 : Data used to calculate the AEP of 30°-90° configuration with 30-degree intervals.

Config. Direction	Wind Direction	10 Minute Data Count Overall (Wind Frequency)	10 minute data count for wind direction	Ratio	AEP [kWh]	AEP Induced [kWh]
30-60	15-45	66356	15099	0.227545	2655	604.1329
60-90	45-75	66356	12713	0.191588	2388	457.5117
90-120	75-105	66356	5510	0.083037	389	32.30137
120-150	105-135	66356	4779	0.072021	804	57.90458
150-180	135-165	66356	3073	0.046311	627	29.03688
180-210	165-195	66356	4940	0.074447	2270	168.9945
210-240	195-225	66356	2602	0.039213	1416	55.52523
240-270	225-255	66356	2472	0.037254	714	26.59907
270-300	255-285	66356	5476	0.082525	830	68.49539
300-330	285-315	66356	3670	0.055308	179	9.900084
330-360	315-345	66356	2853	0.042995	117	5.030457
0-30	345-15	66356	3169	0.047758	425	20.29696
AEP for an isolated turbine [kWh] and all directions accounted for		1495	**Total AEP Induced [kWh]**		1535.729128	

Table A. 7 : Data used to calculate the AEP of 90°-150° configuration with 30-degree intervals.

Config. Direction	Wind Direction	10 Minute Data Count Overall (Wind Frequency)	10 minute data count for wind direction	Ratio	AEP [kWh]	AEP Induced [kWh]
90-120	15-45	66356	15099	0.227545	3104	706.3008
120-150	45-75	66356	12713	0.191588	2510	480.8854
150-180	75-105	66356	5510	0.083037	357	29.64419
180-210	105-135	66356	4779	0.072021	892	64.24239
210-240	135-165	66356	3073	0.046311	590	27.32338
240-270	165-195	66356	4940	0.074447	2021	150.4572
270-300	195-225	66356	2602	0.039213	1630	63.91675
300-330	225-255	66356	2472	0.037254	771	28.72253
330-360	255-285	66356	5476	0.082525	762	62.88372
0-30	285-315	66356	3670	0.055308	175	9.678853
30-60	315-345	66356	2853	0.042995	110	4.729489
60-90	345-15	66356	3169	0.047758	388	18.52993
AEP for an isolated turbine [kWh] and all directions accounted for		1495	**Total AEP Induced [kWh]**		1647.314636	

Table A. 8 : Data used to calculate the AEP of 150°-210° configuration with 30-degree intervals.

Config. Direction	Wind Direction	10 Minute Data Count Overall (Wind Frequency)	10 minute data count for wind direction	Ratio	AEP [kWh]	AEP Induced [kWh]
150-180	15-45	66356	15099	0.227545	2844	647.139
180-210	45-75	66356	12713	0.191588	2783	533.1888
210-240	75-105	66356	5510	0.083037	336	27.90042
240-270	105-135	66356	4779	0.072021	793	57.11235
270-300	135-165	66356	3073	0.046311	680	31.49135
300-330	165-195	66356	4940	0.074447	2184	162.5921
330-360	195-225	66356	2602	0.039213	1497	58.70146
0-30	225-255	66356	2472	0.037254	752	28.01471
30-60	255-285	66356	5476	0.082525	715	59.00506
60-90	285-315	66356	3670	0.055308	160	8.849237
90-120	315-345	66356	2853	0.042995	128	5.503406
120-150	345-15	66356	3169	0.047758	408	19.48508
AEP for an isolated turbine [kWh] and all directions accounted for		1495	**Total AEP Induced [kWh]**		1638.983001	

Table A. 9 : Data used to calculate the AEP of 210°-270° configuration with 30-degree intervals.

Config. Direction	Wind Direction	10 Minute Data Count Overall (Wind Frequency)	10 minute data count for wind direction	Ratio	AEP [kWh]	AEP Induced [kWh]
210-240	15-45	66356	15099	0.227545	2680	609.8216
240-270	45-75	66356	12713	0.191588	2477	474.563
270-300	75-105	66356	5510	0.083037	387	32.1353
300-330	105-135	66356	4779	0.072021	858	61.79369
330-360	135-165	66356	3073	0.046311	624	28.89794
0-30	165-195	66356	4940	0.074447	2130	158.5719
30-60	195-225	66356	2602	0.039213	1403	55.01546
60-90	225-255	66356	2472	0.037254	688	25.63048
90-120	255-285	66356	5476	0.082525	835	68.90801
120-150	285-315	66356	3670	0.055308	168	9.291699
150-180	315-345	66356	2853	0.042995	118	5.073452
180-210	345-15	66356	3169	0.047758	452	21.58641
AEP for an isolated turbine [kWh] and all directions accounted for		1495	**Total AEP Induced [kWh]**		1551.288941	

Table A. 10 : Data used to calculate the AEP of 260°-320° configuration with 30-degree intervals.

Config. Direction	Wind Direction	10 Minute Data Count Overall (Wind Frequency)	10 minute data count for wind direction	Ratio	AEP [kWh]	AEP Induced [kWh]
260-290	15-45	66356	15099	0.227545	3083	701.5223
290-320	45-75	66356	12713	0.191588	2765	529.7403
320-350	75-105	66356	5510	0.083037	355	29.47812
350-20	105-135	66356	4779	0.072021	765	55.09577
20-50	135-165	66356	3073	0.046311	673	31.16717
50-80	165-195	66356	4940	0.074447	1872	139.3646
80-110	195-225	66356	2602	0.039213	1587	62.2306
110-140	225-255	66356	2472	0.037254	753	28.05196
140-170	255-285	66356	5476	0.082525	767	63.29634
170-200	285-315	66356	3670	0.055308	187	10.34255
200-230	315-345	66356	2853	0.042995	120	5.159443
230-260	345-15	66356	3169	0.047758	385	18.38666
AEP for an isolated turbine [kWh] and all directions accounted for		1495	**Total AEP Induced [kWh]**		1673.83587	

Table A. 11 : Data used to calculate the AEP of 30°-90° configuration with 15-degree intervals.

Config. Direction	Wind Direction	10 Minute Data Count Overall (Wind Frequency)	10 minute data count for wind direction	Ratio	AEP [kWh]	AEP Induced [kWh]
30-45	15-30	66488	5060	0.076104	2170	165.1456
45-60	30-45	66488	9750	0.146643	2919	428.0509
60-75	45-60	66488	8607	0.129452	2860	370.2325
75-90	60-75	66488	4106	0.061756	1375	84.91382
90-105	75-90	66488	2732	0.04109	450	18.49055
105-120	90-105	66488	2778	0.041782	294	12.2839
120-135	105-120	66488	2844	0.042775	898	38.41162
135-150	120-135	66488	1935	0.029103	670	19.49901
150-165	135-150	66488	1548	0.023282	325	7.566779
165-180	150-165	66488	1525	0.022936	889	20.39052
180-195	165-180	66488	2348	0.035315	2142	75.64397
195-210	180-195	66488	2592	0.038984	2348	91.53556
210-225	195-210	66488	1638	0.024636	1958	48.23734
225-240	210-225	66488	964	0.014499	707	10.25069
240-255	225-240	66488	1008	0.015161	563	8.535435
255-270	240-255	66488	1464	0.022019	824	18.14367
270-285	255-270	66488	2891	0.043482	974	42.35101
285-300	270-285	66488	2585	0.038879	664	25.81579
300-315	285-300	66488	1783	0.026817	277	7.428273
315-330	300-315	66488	1887	0.028381	80	2.270485
330-345	315-330	66488	1708	0.025689	118	3.031284
345-360	330-345	66488	1145	0.017221	105	1.808221
0-15	345-360	66488	1274	0.019161	103	1.973619
15-30	0-15	66488	2316	0.034833	719	25.04518
AEP for an isolated turbine [kWh] and all directions accounted for		1495	**Total AEP Induced [kWh]**		1527.055754	

Table A. 12 : Data used to calculate the AEP of 90°-150° configuration with 15-degree intervals.

Config. Direction	Wind Direction	10 Minute Data Count Overall (Wind Frequency)	10 minute data count for wind direction	Ratio	AEP [kWh]	AEP Induced [kWh]
90-105	15-30	66488	5060	0.076104	2393	182.1168
105-120	30-45	66488	9750	0.146643	3628	532.0208
120-135	45-60	66488	8607	0.129452	3169	410.2332
135-150	60-75	66488	4106	0.061756	1365	84.29626
150-165	75-90	66488	2732	0.04109	429	17.62766
165-180	90-105	66488	2778	0.041782	260	10.86331
180-195	105-120	66488	2844	0.042775	997	42.64631
195-210	120-135	66488	1935	0.029103	751	21.85635
210-225	135-150	66488	1548	0.023282	307	7.147696
225-240	150-165	66488	1525	0.022936	837	19.19783
240-255	165-180	66488	2348	0.035315	1779	62.82475
255-270	180-195	66488	2592	0.038984	2223	86.6625
270-285	195-210	66488	1638	0.024636	2246	55.33251
285-300	210-225	66488	964	0.014499	816	11.83107
300-315	225-240	66488	1008	0.015161	663	10.0515
315-330	240-255	66488	1464	0.022019	823	18.12165
330-345	255-270	66488	2891	0.043482	895	38.91597
345-360	270-285	66488	2585	0.038879	609	23.67743
0-15	285-300	66488	1783	0.026817	238	6.382415
15-30	300-315	66488	1887	0.028381	85	2.41239
30-45	315-330	66488	1708	0.025689	112	2.877151
45-60	330-345	66488	1145	0.017221	96	1.653231
60-75	345-360	66488	1274	0.019161	100	1.916135
75-90	0-15	66488	2316	0.034833	640	22.29335
AEP for an isolated turbine [kWh] and all directions accounted for		1495	**Total AEP Induced [kWh]**		1672.958218	

Table A. 13 : Data used to calculate the AEP of 150°-210° configuration with 15-degree intervals.

Config. Direction	Wind Direction	10 Minute Data Count Overall (Wind Frequency)	10 minute data count for wind direction	Ratio	AEP [kWh]	AEP Induced [kWh]
150-165	15-30	66488	5060	0.076104	2281	173.5931
165-180	30-45	66488	9750	0.146643	3209	470.5774
180-195	45-60	66488	8607	0.129452	3519	455.5413
195-210	60-75	66488	4106	0.061756	1531	94.54768
210-225	75-90	66488	2732	0.04109	405	16.6415
225-240	90-105	66488	2778	0.041782	245	10.23658
240-255	105-120	66488	2844	0.042775	828	35.4174
255-270	120-135	66488	1935	0.029103	711	20.69223
270-285	135-150	66488	1548	0.023282	352	8.195404
285-300	150-165	66488	1525	0.022936	966	22.15663
300-315	165-180	66488	2348	0.035315	2095	73.98418
315-330	180-195	66488	2592	0.038984	2218	86.46757
330-345	195-210	66488	1638	0.024636	2064	50.84875
345-360	210-225	66488	964	0.014499	749	10.85964
0-15	225-240	66488	1008	0.015161	569	8.626399
15-30	240-255	66488	1464	0.022019	879	19.35471
30-45	255-270	66488	2891	0.043482	856	37.22019
45-60	270-285	66488	2585	0.038879	556	21.61683
60-75	285-300	66488	1783	0.026817	230	6.16788
75-90	300-315	66488	1887	0.028381	76	2.156961
90-105	315-330	66488	1708	0.025689	124	3.185417
105-120	330-345	66488	1145	0.017221	119	2.049317
120-135	345-360	66488	1274	0.019161	111	2.12691
135-150	0-15	66488	2316	0.034833	635	22.11918
AEP for an isolated turbine [kWh] and all directions accounted for		1495	**Total AEP Induced [kWh]**		1654.383242	

Table A. 14 : Data used to calculate the AEP of 210°-270° configuration with 15-degree intervals.

Config. Direction	Wind Direction	10 Minute Data Count Overall (Wind Frequency)	10 minute data count for wind direction	Ratio	AEP [kWh]	AEP Induced [kWh]
210-225	15-30	66488	5060	0.076104	2152	163.7757
225-240	30-45	66488	9750	0.146643	3020	442.8619
240-255	45-60	66488	8607	0.129452	2923	378.388
255-270	60-75	66488	4106	0.061756	1449	89.48373
270-285	75-90	66488	2732	0.04109	464	19.06582
285-300	90-105	66488	2778	0.041782	283	11.8243
300-315	105-120	66488	2844	0.042775	975	41.70527
315-330	120-135	66488	1935	0.029103	710	20.66313
330-345	135-150	66488	1548	0.023282	323	7.520214
345-360	150-165	66488	1525	0.022936	886	20.32171
0-15	165-180	66488	2348	0.035315	1798	63.49573
15-30	180-195	66488	2592	0.038984	2372	92.47118
30-45	195-210	66488	1638	0.024636	1974	48.63151
45-60	210-225	66488	964	0.014499	683	9.902719
60-75	225-240	66488	1008	0.015161	551	8.353507
75-90	240-255	66488	1464	0.022019	782	17.21887
90-105	255-270	66488	2891	0.043482	945	41.09005
105-120	270-285	66488	2585	0.038879	691	26.86552
120-135	285-300	66488	1783	0.026817	255	6.838302
135-150	300-315	66488	1887	0.028381	75	2.12858
150-165	315-330	66488	1708	0.025689	118	3.031284
165-180	330-345	66488	1145	0.017221	105	1.808221
180-195	345-360	66488	1274	0.019161	123	2.356846
195-210	0-15	66488	2316	0.034833	712	24.80135
AEP for an isolated turbine [kWh] and all directions accounted for		1495	**Total AEP Induced [kWh]**		1544.603417	

Table A. 15 : Data used to calculate the AEP of 260°-320° configuration with 15-degree intervals.

Config. Direction	Wind Direction	10 Minute Data Count Overall (Wind Frequency)	10 minute data count for wind direction	Ratio	AEP [kWh]	AEP Induced [kWh]
260-275	15-30	66488	5060	0.076104	2493	189.7272
275-290	30-45	66488	9750	0.146643	3451	506.065
290-305	45-60	66488	8607	0.129452	3276	424.0845
305-320	60-75	66488	4106	0.061756	1595	98.50003
320-335	75-90	66488	2732	0.04109	427	17.54548
335-350	90-105	66488	2778	0.041782	260	10.86331
350-5	105-120	66488	2844	0.042775	837	35.80237
5-20	120-135	66488	1935	0.029103	655	19.06246
20-35	135-150	66488	1548	0.023282	375	8.730899
35-50	150-165	66488	1525	0.022936	813	18.64735
50-65	165-180	66488	2348	0.035315	1664	58.76357
65-80	180-195	66488	2592	0.038984	2029	79.09951
80-95	195-210	66488	1638	0.024636	2144	52.81964
95-110	210-225	66488	964	0.014499	808	11.71508
110-125	225-240	66488	1008	0.015161	645	9.778607
125-140	240-255	66488	1464	0.022019	797	17.54915
140-155	255-270	66488	2891	0.043482	908	39.48123
155-170	270-285	66488	2585	0.038879	608	23.63855
170-185	285-300	66488	1783	0.026817	251	6.731034
185-200	300-315	66488	1887	0.028381	92	2.611058
200-215	315-330	66488	1708	0.025689	126	3.236795
215-230	330-345	66488	1145	0.017221	99	1.704894
230-245	345-360	66488	1274	0.019161	98	1.877813
245-260	0-15	66488	2316	0.034833	638	22.22368
AEP for an isolated turbine [kWh] and all directions accounted for		1495	**Total AEP Induced [kWh]**		1660.259205	

APPENDIX B

Table B. 16 : Angular intervals with the corresponding power coefficient values used in analyses for 30°-90°, 90°-150°, 150°-210° and 210°-270° configurations.

15 Degree Intervals		30 Degree Intervals		60 Degree Intervals	
Angular Interval	**Power Coefficient**	**Angular Interval**	**Power Coefficient**	**Angular Interval**	**Power Coefficient**
0-15	1	0-30	1.09373	30-90	0.968839
15-30	1.15765	30-60	0.93747	90-150	1.076424
30-45	0.95664	60-90	1.00021	150-210	1.112938
45-60	0.91255	90-120	1.09601	210-270	0.993947
60-75	0.96835	120-150	1.05124	270-330	1.106963
75-90	1.02942	150-180	1.00416	330-30	1.051764
90-105	1.0551	180-210	1.16566		
105-120	1.13399	210-240	0.94621		
120-135	1.07311	240-270	1.03734		
135-150	1.02209	270-300	1.08893		
150-165	1.00534	300-330	1.12139		
165-180	1.00298	330-360	1		
180-195	1.19152				
195-210	1.14626				
210-225	0.94845				
225-240	0.94397				
240-255	0.98977				
255-270	1.08491				
270-285	1.08833				
285-300	1.08952				
300-315	1.16549				
315-330	1.08281				
330-345	1				
345-360	1				

Table B. 17 : Angular intervals with the corresponding power coefficient values used in analyses for 260°-320° configuration

15 Degree Intervals		30 Degree Intervals		60 Degree Intervals	
Angular Interval	Power Coefficient	Angular Interval	Power Coefficient	Angular Interval	Power Coefficient
0-15	1	0-30	1.09373	30-90	0.968839
15-30	1.15765	30-60	0.93747	90-150	1.076424
30-45	0.95664	60-90	1.00021	150-210	1.112938
45-60	0.91255	90-120	1.09601	210-270	0.993947
60-75	0.96835	120-150	1.05124	270-330	1.106963
75-90	1.02942	150-180	1.00416	330-30	1.051764
90-105	1.0551	180-210	1.16566		
105-120	1.13399	210-240	0.94621		
120-135	1.07311	240-270	1.03734		
135-150	1.02209	270-300	1.08893		
150-165	1.00534	300-330	1.12139		
165-180	1.00298	330-360	1		
180-195	1.19152				
195-210	1.14626				
210-225	0.94845				
225-240	0.94397				
240-255	0.98977				
255-270	1.08491				
270-285	1.08833				
285-300	1.08952				
300-315	1.16549				
315-330	1.08281				
330-345	1				
345-360	1				

APPENDIX C

Table C. 18 : Power generation of the sample turbine with corresponding wind speed.

WIND SPEED	POWER GENERATION[KW]
4.192579073	0.017703163
4.204629289	0.018185172
4.221610175	0.018864407
4.234394182	0.019375767
4.249638043	0.019985522
4.263902785	0.020556111
4.283544239	0.02134177
4.30329542	0.022131817
4.323046602	0.022921864
4.343785344	0.023751414
4.365511643	0.025489518
4.387237943	0.02635857
4.408964244	0.027227622
4.430690543	0.027227622
4.452416843	0.028096674
4.474143144	0.028965726
4.495869443	0.029834778
4.537306194	0.031492248
4.582975894	0.033319036
4.628666913	0.035146677
4.67445777	0.036978311
4.720248626	0.038809945
4.766039482	0.040641579
4.81183034	0.042473214
4.857621196	0.044304848
4.903412054	0.046136482
4.94920291	0.047968116
5.01125401	0.051437447
5.120753433	0.059685669
5.253727181	0.070298175
5.387926667	0.081034133
5.55295308	0.094236246

Table C. 19 (continued): Power generation of the sample turbine with corresponding wind speed.

|	
5.790765698	0.113261256
6.025045027	0.132870178
6.214195531	0.151419553
6.398567325	0.169856732
8.160745208	0.445363946
8.787866672	0.589088001
9.06924039	0.656617694
9.282559249	0.70781422
9.491157638	0.757877833
9.677279254	0.802547021
9.854218951	0.8445948
10.02290843	0.883665349
10.13145745	0.901033192
10.24000647	0.918401035
10.34855548	0.935768877
10.4571045	0.95313672
10.5782069	0.968776876
10.70124977	0.984149972
10.82665245	0.999198294
10.95287616	1.013500917
11.080593	1.02644744
11.2110715	1.03688572
11.34155	1.047324
11.47709972	1.057601889
11.62540906	1.067476217
11.78384022	1.077030413
11.9427988	1.086567928
12.04893394	1.078148016
12.13517487	1.062965025
12.21759102	1.046481796
12.30000717	1.029998566
12.37867714	1.014264573
12.45385965	0.999315953
12.5485263	0.987088422
12.67527882	0.979483271
12.76733371	0.973959977
12.86876207	0.979719672
12.97069054	0.966430398
13.13678761	0.968207257
13.32075075	0.97924259
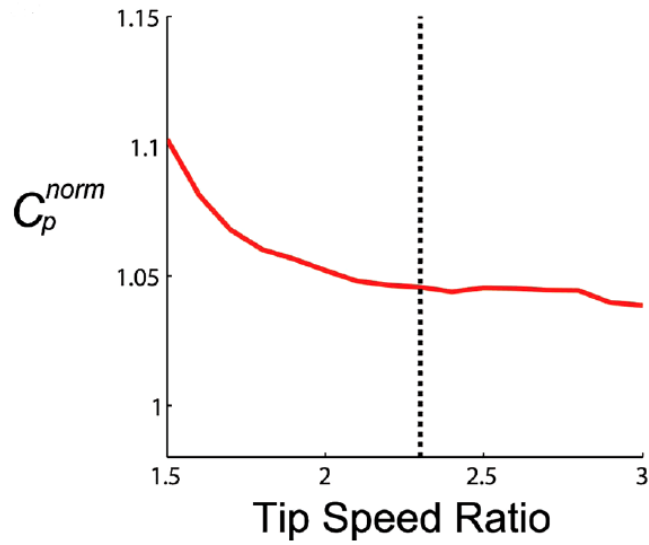
Figure C.1 : Plot of normalized power coefficient, C_p^{norm}, versus tip speed ratio for all incident wind directions [4].

Using Figure C.1 from [4] and NREL's power curve for the sample turbine [12], Table A.12 has been derived in order to get the same operational power range that is used in Dabiri's study [4]. The data gathered with a series of interpolations.

APPENDIX D

Table D.19 shows the new turbine power curve data sector-wise. This table created with multiplication of power coefficient values from Table B.17 (60 degree intervals) by power generation values from Table C.18. Data in this table used in Turbine Editor tool of WAsP to create new turbine power curves as in Figure 3.3.

Table D. 20 : A sample representation of new power generation values of the paired VAWT sector-wise.

Interpolation Data		Sectors (Angular Intervals)					
		Power					
Wind Speed	Power (Isolated)	260-320	320-20	20-80	80-140	140-200	200-260
4.19258	0.0177	0.01993	0.0177	0.01827	0.01907	0.01957	0.01792
4.20463	0.01819	0.02047	0.01819	0.01876	0.01959	0.0201	0.0184
4.22161	0.01886	0.02124	0.01886	0.01946	0.02032	0.02085	0.01909
4.23439	0.01938	0.02181	0.01938	0.01999	0.02087	0.02142	0.01961
4.24964	0.01999	0.0225	0.01999	0.02062	0.02153	0.02209	0.02023
4.2639	0.02056	0.02314	0.02056	0.02121	0.02214	0.02272	0.0208
4.28354	0.02134	0.02403	0.02134	0.02202	0.02299	0.02359	0.0216
4.3033	0.02213	0.02491	0.02213	0.02283	0.02384	0.02446	0.0224
4.32305	0.02292	0.0258	0.02292	0.02365	0.02469	0.02534	0.0232
4.34379	0.02375	0.02674	0.02375	0.02451	0.02558	0.02625	0.02404
4.36551	0.02549	0.02869	0.02549	0.0263	0.02746	0.02818	0.0258
4.38724	0.02636	0.02967	0.02636	0.0272	0.02839	0.02914	0.02667
4.40896	0.02723	0.03065	0.02723	0.02809	0.02933	0.0301	0.02755
4.43069	0.02723	0.03065	0.02723	0.02809	0.02933	0.0301	0.02755
4.45242	0.0281	0.03163	0.0281	0.02899	0.03027	0.03106	0.02843
4.47414	0.02897	0.03261	0.02897	0.02989	0.0312	0.03202	0.02931
4.49587	0.02983	0.03359	0.02983	0.03078	0.03214	0.03298	0.03019
4.53731	0.03149	0.03545	0.03149	0.03249	0.03392	0.03481	0.03187
4.58298	0.03332	0.03751	0.03332	0.03438	0.03589	0.03683	0.03372
4.62867	0.03515	0.03957	0.03515	0.03626	0.03786	0.03885	0.03557
4.67446	0.03698	0.04163	0.03698	0.03815	0.03983	0.04088	0.03742
4.72025	0.03881	0.04369	0.03881	0.04004	0.04181	0.0429	0.03928
4.76604	0.04064	0.04575	0.04064	0.04193	0.04378	0.04492	0.04113
4.81183	0.04247	0.04781	0.04247	0.04382	0.04575	0.04695	0.04298
4.85762	0.0443	0.04988	0.0443	0.04571	0.04772	0.04897	0.04484

Table D. 21 (continued): A sample representation of new power generation values of the paired VAWT sector-wise.

4.90341	0.04614	0.05194	0.04614	0.0476	0.0497	0.051	0.04669
4.9492	0.04797	0.054	0.04797	0.04949	0.05167	0.05302	0.04854
5.01125	0.05144	0.05791	0.05144	0.05307	0.05541	0.05686	0.05205
5.12075	0.05969	0.06719	0.05969	0.06158	0.06429	0.06598	0.0604
5.25373	0.0703	0.07914	0.0703	0.07253	0.07572	0.07771	0.07114
5.38793	0.08103	0.09122	0.08103	0.08361	0.08729	0.08957	0.08201
5.55295	0.09424	0.10609	0.09424	0.09723	0.10151	0.10417	0.09537
5.79077	0.11326	0.1275	0.11326	0.11686	0.122	0.1252	0.11462
6.02505	0.13287	0.14958	0.13287	0.13709	0.14312	0.14687	0.13446
6.2142	0.15142	0.17046	0.15142	0.15623	0.16311	0.16738	0.15324
6.39857	0.16986	0.19122	0.16986	0.17525	0.18297	0.18776	0.17189
8.16075	0.44536	0.50137	0.44536	0.4595	0.47973	0.4923	0.45071
8.78787	0.58909	0.66317	0.58909	0.60779	0.63455	0.65117	0.59615
9.06924	0.65662	0.73919	0.65662	0.67747	0.70729	0.72582	0.66449
9.28256	0.70781	0.79682	0.70781	0.73029	0.76244	0.78241	0.7163
9.49116	0.75788	0.85318	0.75788	0.78194	0.81637	0.83775	0.76697
9.67728	0.80255	0.90347	0.80255	0.82803	0.86448	0.88713	0.81217
9.85422	0.84459	0.9508	0.84459	0.87141	0.90978	0.93361	0.85472
10.0229	0.88367	0.99479	0.88367	0.91172	0.95186	0.9768	0.89426
10.1315	0.90103	1.01434	0.90103	0.92964	0.97057	0.996	0.91184
10.24	0.9184	1.03389	0.9184	0.94756	0.98928	1.01519	0.92942
10.3486	0.93577	1.05344	0.93577	0.96548	1.00799	1.03439	0.94699
10.4571	0.95314	1.073	0.95314	0.9834	1.02669	1.05359	0.96457
10.5782	0.96878	1.0906	0.96878	0.99954	1.04354	1.07088	0.9804
10.7012	0.98415	1.10791	0.98415	1.0154	1.0601	1.08787	0.99595
10.8267	0.9992	1.12485	0.9992	1.03092	1.07631	1.10451	1.01118
10.9529	1.0135	1.14095	1.0135	1.04568	1.09172	1.12032	1.02566
11.0806	1.02645	1.15553	1.02645	1.05904	1.10566	1.13463	1.03876
11.2111	1.03689	1.16728	1.03689	1.06981	1.11691	1.14617	1.04932
11.3416	1.04732	1.17903	1.04732	1.08058	1.12815	1.15771	1.05989
11.4771	1.0576	1.1906	1.0576	1.09118	1.13922	1.16907	1.07029
11.6254	1.06748	1.20171	1.06748	1.10137	1.14986	1.17998	1.08028
11.7838	1.07703	1.21247	1.07703	1.11123	1.16015	1.19054	1.08995
11.9428	1.08657	1.22321	1.08657	1.12107	1.17042	1.20109	1.0996
12.0489	1.07815	1.21373	1.07815	1.11238	1.16135	1.19178	1.09108
12.1352	1.06297	1.19664	1.06297	1.09672	1.145	1.175	1.07571
12.2176	1.04648	1.17808	1.04648	1.07971	1.12724	1.15677	1.05903
12.3	1.03	1.15952	1.03	1.0627	1.10949	1.13855	1.04235
12.3787	1.01426	1.14181	1.01426	1.04647	1.09254	1.12116	1.02643
12.4539	0.99932	1.12498	0.99932	1.03105	1.07644	1.10464	1.0113

Table D. 22 (continued): A sample representation of new power generation values of the paired VAWT sector-wise.

12.5485	0.98709	1.11122	0.98709	1.01843	1.06327	1.09112	0.99893
12.6753	0.97948	1.10266	0.97948	1.01058	1.05507	1.08271	0.99123
12.7673	0.97396	1.09644	0.97396	1.00488	1.04912	1.07661	0.98564
12.8688	0.97972	1.10292	0.97972	1.01083	1.05533	1.08298	0.99147
12.9707	0.96643	1.08796	0.96643	0.99712	1.04101	1.06829	0.97802
13.1368	0.96821	1.08996	0.96821	0.99895	1.04293	1.07025	0.97982
13.3208	0.97924	1.10238	0.97924	1.01033	1.05481	1.08245	0.99099

CURRICULUM VITAE

FERHAT CEM BAŞER

Mechanical Engineer

PERSONAL INFO

Birth Place: ISTANBUL

Date of Birth: 29.04.1992

Adress: Atatürk Mh. 202/5 Sk. No:40 Maviyaka Sitesi B Blok D:14 Buca/Izmir/Turkey

Phone Number: +905354039012

E-mail: frhtcm@gmail.com

Military Occupation: Completed

EDUCATION

-İzmir Katip Çelebi University (İzmir/Turkey)

Master's Degree in Mechanical Engineering   2017-......

-Dokuz Eylül University (İzmir/Turkey)

Bachelor's Degree in Mechanical Engineering (GPA: 2.6/4)   2011-2017

-Akyazı Anatolian High School, SAKARYA   2006-2010

-Münir Nurettin Selçuk Elemantary School, İSTANBUL   2001-2006

-Birikim Koleji Elemantary School, İSTANBUL   1998-2001

CERTIFICATES AND WORKSHOPS

-TMMOB UCTEA Chamber of Mechanical Engineers

"ISO:9001:2015 Fundamentals Seminar" (16 hours)   2017

"Lean Manufacturing Techniques Seminar"(8 hours)   2017

"FMEA Seminar" (8 hours)   2017

"PDCA Seminar" (8 hours)   2017

"Project Management Methodology Seminar" (8 hours)   2017

"Wind Energy Plant Training" (15 hours)   2019

INTERNSHIPS

-Metyx Composites - Telateks A.Ş.

Profession Internship (Mandatory internship, 25 work days) 2017

-Yıldız Sfero ve Pik Döküm San.Tic.Ltd.Şti.

Casting Internship (Mandatory internship, 10 work days)   2016

-Beşer Balatacılık San.Tic.A.Ş.

Machining Internship (Mandatory internship, 15 work days) 2016

EXPERIENCE

Metyx Composites - Telateks A.Ş. Manisa-TURKEY   July-September 2014
General Assistant

- Designed nesting schemes of composite wind turbine rotor blade kits using CAD/CAM softwares

- Worked as a quality control assistant

PROJECTS AND STUDY GROUPS

- Analysis of Photovoltaic/Thermal Hybrid Systems Using ANSYS/FLUENT

Bachelor's Degree Graduation Thesis

- Estimation of annual energy production of coupled vertical-axis wind turbines in a semi-complex terrain

Master's Degree Graduation Thesis

- Izmir Katip Çelebi University Wind Turbine Research Group

Numerical and Field Study of Vertical Axis Wind Turbines

LANGUAGE

English: Upper-Intermediate (YDS(Foreign Languages Exam): 81,25/10) April 2017

COMPUTER SKILLS

AutoCAD, SolidWorks, WAsP, WindPRO, Ansys/Fluent, MS Office

REFERENCES

Dr. Ziya Haktan Karadeniz / İzmir Katip Çelebi University, Faculty of Mechanical Engineering

(zhaktan.karadeniz@ikc.edu.tr : +905055250863)

Associate Prof. Dr. Levent Çetin / İzmir Katip Çelebi University, Faculty of Engineering, Mechatronic Engineering

(levent.cetin@ikc.edu.tr : +905327350444)

Associate Prof. Dr. Mehmet Akif EZAN / İzmir Dokuz Eylül University, Faculty of Engineering, Mechanical Engineering

(mehmetezan@gmail.com : +905055176237)

Mechanical Eng. Msc. İskender Kökey / XGEN Energy Managing Partner

(iskender.kokey@xgen.com.tr : +905327323509)

SOCIAL

www.linkedin.com/in/fcbaser

List of Publications:

Conference Papers

- Başer F.C., Kökey İ., Karadeniz Z.H., Turgut A., Estimation of annual energy production of coupled counter-rotating vertical-axis wind turbines in a semi-complex terrain, IMSEC 2019 - 4th International Mediterranean Science and Engineering Congress, April 25-27, 2019 – Antalya/TURKEY